

# Understanding Read Disturbance in High Bandwidth Memory: An Experimental Analysis of Real HBM2 DRAM Chips

Ataberk Olgun   Majd Osseiran   Abdullah Giray Yaglikci   Yahya Can Tugrul  
Haocong Luo   Steve Rhyner   Behzad Salami   Juan Gomez Luna   Onur Mutlu

ETH Zurich

*DRAM read disturbance is a significant and worsening safety, security, and reliability issue of modern DRAM chips that can be exploited to break memory isolation. Therefore, it is important to understand real DRAM chips' read disturbance characteristics. Two prominent examples of read-disturb phenomena are RowHammer and RowPress. Many existing DRAM modules of various form factors (e.g., DDR4) are vulnerable to RowHammer and RowPress. Unfortunately, no prior work extensively studies RowHammer and RowPress in modern high-bandwidth memory (HBM) chips, which are commonly used in modern GPUs and FPGAs. In this work, we experimentally demonstrate the effects of read disturbance and uncover the inner workings of undocumented in-DRAM read disturbance mitigation mechanisms in High Bandwidth Memory (HBM).*

*Our detailed characterization of six real HBM2 DRAM chips shows that (1) the number of read disturbance errors (i.e., bitflips) and the number of row activations needed to induce the first read disturbance bitflip significantly varies between different HBM2 chips and different 3D-stacked channels, pseudo channels, banks, and rows inside an HBM2 chip. We observe that the variation in the average number of bitflips per DRAM row is more prominent across channels in some HBM2 chips than across all channels in all HBM2 chips. (2) The DRAM rows at the end and in the middle of a DRAM bank exhibit significantly fewer read disturbance bitflips than the rest of the rows. (3) It takes fewer additional activations to induce more read disturbance bitflips in a DRAM row if the row exhibits the first bitflip already at a relatively high activation count. (4) HBM2 chips exhibit read disturbance bitflips with only two row activations when rows are kept active for an extremely long time.*

*We show that a modern HBM2 DRAM chip implements undocumented read disturbance defenses that can track potential aggressor rows based on how many times they are activated, and refresh their victim rows with every 17 periodic refresh operations. We draw key takeaways from our observations and discuss their implications for future read disturbance attacks and defenses. We explain how our findings could be leveraged to develop both i) more powerful read disturbance attacks and ii) more efficient read disturbance defense mechanisms.*

## 1. Introduction

Modern DRAM chips suffer from read disturbance [1–4] issues that can be exploited to break memory isolation, threatening the safety, security, and reliability of modern DRAM-based computing systems. RowHammer [1] and RowPress [4]

are two prominent examples of read disturbance. Repeatedly opening/activating and closing a DRAM row (i.e., aggressor row) many times (e.g., tens of thousands) induces RowHammer bitflips in physically nearby rows (i.e., victim rows). Keeping the aggressor row open for a long period of time (i.e., a large aggressor row on time,  $t_{AggON}$ ) amplifies the effects of read disturbance and induces RowPress bitflips, without many repeated aggressor row activations [4]. Numerous studies demonstrate that a malicious attacker can reliably cause read disturbance bitflips in a targeted manner to compromise system integrity, confidentiality, and availability [1, 5–67]. Read disturbance worsens in new DRAM chips with smaller technology nodes, where RowHammer bitflips 1) happen with fewer row activations, e.g.,  $10\times$  reduction in less than a decade [68] and 2) appear in more DRAM cells, compared to old DRAM chips [3, 27, 35, 38, 68–71].

To meet the high-bandwidth requirements of modern data-intensive applications (e.g., GPU workloads [72, 73]), DRAM designers develop High Bandwidth Memory (HBM) [74] DRAM chips, which contain multiple layers of 3D-stacked DRAM dies, using cutting-edge technology nodes.<sup>1</sup> It is important to understand read disturbance in HBM DRAM chips that have new architectural characteristics (e.g., multiple layers of DRAM dies, area- and energy-intensive through-silicon vias), which might affect the chip's read disturbance vulnerability in currently-unknown ways. Such understanding can help identify potential read-disturbance-induced security and reliability issues in HBM-based systems and allow for effective and efficient defense mechanisms.

**Our goal** in this work is to experimentally analyze how vulnerable HBM DRAM chips are to read disturbance. To this end, we provide the first detailed experimental characterization of the RowHammer and the RowPress vulnerability in six modern HBM2 DRAM chips. We provide four main analyses in our study. First, we analyze the spatial variation in RowHammer vulnerability based on the physical location of victim rows in terms of two metrics: the fraction of DRAM cells that experience a bitflip in a DRAM row ( $BER$ ) and the minimum hammer count necessary to cause a RowHammer bitflip ( $HC_{first}$ ) (Section 4). Second, we analyze the number of aggressor row activations (i.e., hammer count) necessary to induce the first 10 bitflips in a DRAM row (Section 5). We demonstrate how many additional hammer count over  $HC_{first}$  is needed to induce

<sup>1</sup>We use “chip” to refer to an HBM2 stack. An HBM2 stack contains one or multiple DRAM layers. We refer to each such layer using “DRAM die”.

each of the first 10 bitflips. Third, we test RowPress and RowHammer’s sensitivities to the amount of time a row remains active, i.e., the aggressor row on time ( $t_{AggON}$ ) (Section 6). To do so, we sweep  $t_{AggON}$  from the minimum standard 29.0 ns to an extreme 16.0 ms. Fourth, we investigate undocumented in-DRAM read disturbance defense mechanisms that are triggered by periodic refresh operations (e.g., TRR [38, 44, 75]) in an HBM2 chip (Section 7).<sup>2</sup> We summarize the key observations from our four main analyses.

**1) Spatial variation in RowHammer (Section 4).** First, DRAM rows near the end and in the middle of a DRAM bank (the last and the middle 832 rows) exhibit substantially smaller  $BER$  than other DRAM rows. Second, RowHammer  $BER$  and  $HC_{first}$  vary between DRAM chips. For example, the chip-level mean  $BER$  and minimum  $HC_{first}$  differ by up to 0.49 (proportionally  $1.6\times$ ) and 3556, respectively. Third, different 3D-stacked channels of an HBM2 chip exhibit significantly different levels of RowHammer vulnerability in  $BER$  (up to  $1.99\times$  difference in highest and lowest mean  $BER$ ) and  $HC_{first}$ . Fourth, the mean  $BER$  variation across channels in multiple HBM2 chips (e.g., the largest mean  $BER$  across all rows in a channel in Chip 4 is 0.88 higher than the smallest) is larger than the mean  $BER$  variation across all HBM2 chips (the largest mean  $BER$  across all rows in a chip is 0.38 higher than the smallest), for all tested data patterns (Table 1).

**2) RowHammer’s Sensitivity to Hammer Count (Section 5).** We show that the hammer count to induce more than one RowHammer bitflip (up to 10) in a row can be very close to ( $1.15\%$  larger than) or very far from ( $5.22\times$  larger than) the hammer count to induce the first RowHammer bitflip depending on the DRAM row. We find that, in general, it takes fewer additional hammer counts (over  $HC_{first}$ ) to induce up to 10 RowHammer bitflips in a DRAM row that has a large  $HC_{first}$  compared to a DRAM row that has a small  $HC_{first}$ .

**3) RowHammer’s and RowPress’s Sensitivities to  $t_{AggON}$  (Section 6).** We observe that as the time an aggressor row remains open ( $t_{AggON}$ ) increases, DRAM cells become more vulnerable to read disturbance such that the  $HC_{first}$  of a row can be reduced by  $222.57\times$  (when  $t_{AggON}$  is  $35.1\mu s$ ) on average and down to 1 for an extreme  $t_{AggON}$  of 16 ms.

**4) In-DRAM RowHammer defenses (Section 7).** We uncover that an HBM2 DRAM chip implements an in-DRAM RowHammer defense mechanism that is not disclosed in the HBM2 specification [74]. The undocumented target row refresh (TRR) mechanism detects i) the *first* row that gets activated after a TRR operation (a victim row refresh) and ii) the row whose activation count exceeds half the number of total row activations within a refresh interval as aggressor rows. We experimentally demonstrate that a careful attacker can practically and reliably defeat this undocumented TRR mechanism in real HBM2 DRAM chips by leveraging our observations.

We highlight 3 of the 6 key implications of our observations

<sup>2</sup>The HBM2 standard specifies a Target Row Refresh (TRR) Mode. To enable TRR Mode, the memory controller issues a well-defined series of commands. We investigate undocumented TRR mechanisms that function even when the DRAM chip is *not* in TRR mode.

for future read disturbance attacks and defenses (Section 8): 1) the maximum  $BER$  (247 bitflips in a row of 8192 bits) is likely sufficient for conducting practical attacks (e.g., privilege escalation) or degrading the lifetime of modern HBM-based systems, 2) a read disturbance attack could find exploitable bitflips faster by targeting the most-read-disturbance-vulnerable HBM2 channels, and 3) read disturbance defense mechanisms could adapt to the heterogeneous distribution of the RowHammer and RowPress vulnerability across channels and subarrays and more efficiently prevent read disturb bitflips.

We make the following contributions:

- We present the first detailed experimental characterization of read disturbance (RowHammer and RowPress) in six state-of-the-art HBM2 DRAM chips. We show that all of the tested HBM2 DRAM chips are susceptible to read disturbance bitflips.
- We show that the RowHammer and RowPress vulnerability in HBM2 varies significantly across chips and HBM2 components within each chip (e.g., 3D-stacked channels, pseudo-channels, banks, and rows).
- We present the first analysis on hammer count to induce up to 10 bitflips in a DRAM row. We show that a DRAM row with a large hammer count to induce the first bitflip is likely to require fewer additional hammer counts to exhibit the next 9 bitflips.
- We characterize the RowPress vulnerability in six HBM2 chips. We show that all chips exhibit bitflips with a hammer count of only one when the aggressor row is kept open for a very long time (16 ms).
- We uncover the inner workings of an undocumented in-HBM-chip read disturbance defense mechanism. We analyze this defense mechanism and craft a specialized RowHammer access pattern that bypasses the defense.

## 2. Background & Motivation

We describe the necessary background on HBM2 organization and operation to explain the RowHammer vulnerability and its implications for real HBM2 systems.

### 2.1. HBM2 Organization

Figure 1 presents the organization of an HBM2 DRAM chip [76] when used in an FPGA-based system. The memory controller communicates with one or multiple stacks of HBM using the HBM2 interface (❶). An HBM2 stack contains multiple DRAM dies stacked on top of the buffer die and connected using through-silicon vias (TSVs) (❷). Each HBM2 die comprises one or multiple HBM2 channels that can operate independently (❸). An HBM2 channel contains multiple pseudo channels and each pseudo channel has multiple banks (❹). A DRAM bank comprises multiple DRAM cells that are laid in a two-dimensional array of rows and columns (❺). DRAM cells are typically partitioned into multiple DRAM subarrays [77–79] (not shown in the figure) that each contain a row buffer. When enabled, a wordline connects a DRAM cell to its bitline, copying the data stored in the DRAM cell to the row buffer.

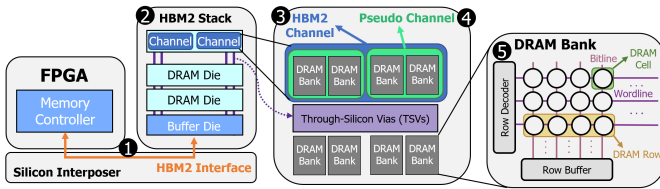


Figure 1: HBM2 DRAM system organization

## 2.2. HBM2 Operation

To access a DRAM chip, the memory controller needs to issue the following sequence of commands. First, the controller issues an activate (ACT) command targeting a DRAM row to access a DRAM cell. The row decoder enables the row’s wordline, copying the data in the row to the row buffer. Second, to read from or write to a particular column in that row, a RD or WR command needs to be issued. Finally, when accesses to the open row are complete, the memory controller issues a precharge (*PRE*) command, which disables the enabled wordline so that the memory controller can later access a different cell in another DRAM row.

To maintain reliable operation of DRAM, the memory controller must adhere to manufacturer-recommended, standard timing parameters between commands. These timing parameters ensure that the DRAM circuitry has enough time to execute the operations dictated by the command. Two relevant timing parameters for our study are charge restoration latency ( $t_{RAS}$ ) and refresh interval ( $t_{REFI}$ ). First,  $t_{RAS}$ , the minimum time that a row should remain active before a *PRE* command is sent to the row’s bank.  $t_{RAS}$  guarantees that DRAM sense amplifiers have enough time to restore charge in cells of the open row before the row is closed. Second, the average periodic interval at which a refresh cycle is required i.e.,  $t_{REFI}$ . Since a DRAM cell stores data as charge in its capacitor and the capacitor naturally loses charge over time, the capacitor must be periodically refreshed to prevent data corruption. Consequently, the memory controller should issue a *REF* command on average every  $3.9 \mu s$  [74] ( $t_{REFI}$ ), such that every DRAM cell is refreshed once at a fixed refresh window (e.g., 32 ms). The memory controller may delay a *REF* command up to  $35.1 \mu s$  ( $9 * t_{REFI}$ ). However any such large delay must be compensated by multiple smaller delays between successive *REF* commands following the large delay.

## 2.3. Motivation

Read-disturb phenomena (e.g., RowHammer [1] and RowPress [4]) break the fundamental building block of modern system security principles, i.e., *memory isolation*. This property allows read-disturb phenomena to be used in system-level attacks that compromise system integrity, confidentiality, and availability in various real computing systems, as many prior works have shown [1, 5–67]. Therefore, it is critical to understand the properties of the RowHammer and RowPress vulnerability to design defense mechanisms and protect modern DRAM chips against read-disturbance-based attacks. Unfortunately, no prior work extensively studies the RowHammer and RowPress vulnerability of modern HBM chips. To this end,

our goal is to evaluate and understand the RowHammer and RowPress vulnerability in real HBM chips. To achieve this goal, we perform a rigorous experimental characterization study of read disturbance on six HBM2 chips in two different types of integrated circuit packages.

## 3. Experimental Infrastructure

We experimentally study 6 HBM2 chips using a modified version of the DRAM Bender testing infrastructure [80, 81]. This infrastructure allows us to precisely control the HBM2 command timings at the granularity of 1.66 ns (i.e., the HBM2 interface clock speed is 600 MHz). All tested HBM2 chips have i) a stack density of 4 GiB, ii) 8 channels, iii) 2 pseudo channels, iv) 16 banks, v) 16384 rows, and vi) 1KB storage in each row.

**Testing setup.** Figure 2 shows one of our six testing setups. We conduct experiments using one Bittware XUPVH [82] (1) and five AMD Xilinx Alveo U50 FPGA boards [83] (not shown in the figure). We use the heating pad (2) and the cooling fan (3) to increase and reduce the temperature of the HBM2 chip, respectively. The Arduino [84] temperature controller (4) communicates with i) the host machine to retrieve a target temperature and ii) the FPGA board to retrieve the HBM2 chip’s temperature. A host machine executes the test programs described in Section 3.1 on the FPGA board using the PCIe connection (5).

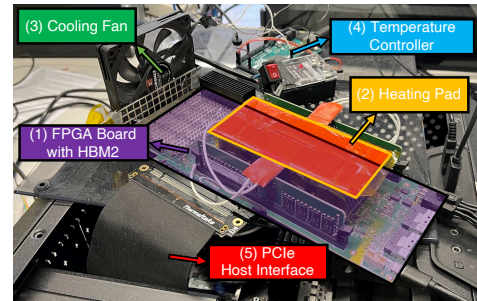


Figure 2: FPGA-based HBM2 DRAM tester.

### 3.1. Testing Methodology

**Disabling Sources of Interference.** We identify four sources that can interfere with our characterization results: 1) periodic refresh [74], 2) on-die read disturbance defense mechanisms (e.g., TRR [38, 44, 75]), 3) data retention failures, and 4) ECC. First, we do *not* issue periodic refresh commands in our experiments. Second, disabling periodic refresh disables all known on-die read disturbance defense mechanisms [44, 68–70]. Third, we ensure that our experiments finish within the 32 ms standard refresh interval where manufacturers guarantee no retention errors will occur [74]. Fourth, we disable ECC by setting the corresponding HBM2 mode register bit to zero [74].

**RowHammer and RowPress Access Pattern.** We use the double-sided read disturbance access pattern [1, 14, 68, 70], which alternately activates each aggressor row neighboring a victim row. We record the bitflips observed on the sandwiched victim row (i.e., the row between two aggressor rows).

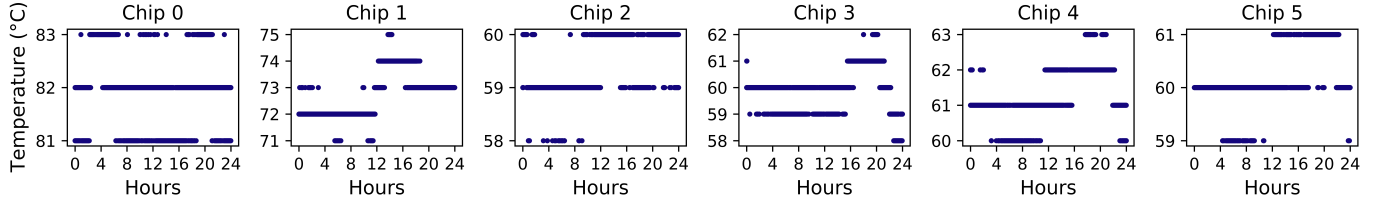


Figure 3: Tested HBM2 chips’ temperature over time (24 hours). We draw temperature measurements taken every 5 seconds over a 24 hour time window.

**Logical-to-Physical Row Mapping.** DRAM manufacturers use mapping schemes to translate logical (memory-controller-visible) addresses to physical row addresses [1, 9, 28, 39, 70, 85–95]. To identify aggressor rows that are physically adjacent to a victim row, we reverse-engineer the logical to physical row mapping scheme following the methodology described in prior work [70].

**RowHammer and RowPress Test Parameters.** We configure our tests by tuning 3 parameters: 1) Hammer count: We define the *hammer count* of a double-sided read disturbance access pattern as the number of activations each aggressor row receives. Therefore, during a double-sided RowHammer or a RowPress test with a hammer count of 1000, we activate each of the two aggressor rows 1000 times, resulting in a total of 2000 row activations. 2)  $t_{AggON}$ : The time each aggressor row stays on every time it is activated during a RowHammer or a RowPress test. 3) Data pattern: We use the four data patterns (Table 1) that are widely used in memory reliability testing [96] and by prior work on DRAM characterization (e.g., [1, 4, 68, 70]). For each DRAM row, we define  $WCDP$  as the data pattern that causes the smallest  $HC_{first}$ . When multiple data patterns cause the lowest  $HC_{first}$ , we select  $WCDP$  as the data pattern that causes the largest  $BER$  at a hammer count of 256K.

Table 1: Data patterns used in our experiments

Row Addresses	Rowstripe0	Rowstripe1	Checkered0	Checkered1
Victim (V)	0x00	0xFF	0x55	0xAA
Aggressors ( $V \pm 1$ )	0xFF	0x00	0xAA	0x55
$V \pm [2:8]$	0x00	0xFF	0x55	0xAA

**RowHammer Vulnerability Metrics.** We measure RowHammer vulnerability based on two metrics: 1)  $HC_{first}$  and 2)  $BER$ .

**Tested DRAM Components.** To maintain a reasonable experiment time, the number of DRAM components (channels, pseudo-channels, banks, and rows) we test vary depending on the experiment type. We describe how many components we test in each of the following sections for our various experiments. Table 2 summarizes the number of components tested for each experiment type.

**HBM2 Chip Labeling.** We use the labels listed in Table 3 to refer to the HBM2 chips on six FPGA boards that we test in the remainder of our paper.

**Temperature Control.** We use the temperature controller setup shown in Figure 2 for Chip 0 and set the target tempera-

Table 2: Tested DRAM components for each experiment type

Experiment Type	Rows (Per Bank)	Banks	Pseudo Channels	Channels
RowHammer $BER$	16384	1	1	8
RowHammer $HC_{first}$	3072	3	2	8
RowPress $BER$	384	1	1	3
RowPress $HC_{first}$	384	1	1	3

Table 3: Labels for the HBM2 chips in each tested FPGA board

FPGA Board	Chip Label
Bittware XUPV VH	Chip 0
AMD Xilinx Alveo U50	Chip 1, 2, 3, 4, 5

ture for this chip to 82 °C. Figure 3 shows how the temperature of each chip (measured by the temperature sensors inside each chip [74]) varies during 24 hours based on measurements taken every 5 seconds. Even though we do not have the same temperature controller setups for the five other chips, we observe that their temperature is stable.

## 4. Spatial Variation in RowHammer

We provide the first detailed spatial variation analysis of RowHammer across channels, pseudo channels, banks, and rows in six HBM2 chips.

### 4.1. RowHammer Across Chips

Figure 4 shows the distribution of  $BER$  (y-axis) across all tested DRAM rows for each tested data pattern (x-axis) in all tested chips (color-coded). A higher  $BER$  indicates worse RowHammer vulnerability as more DRAM cells in a row exhibit RowHammer bitflips.

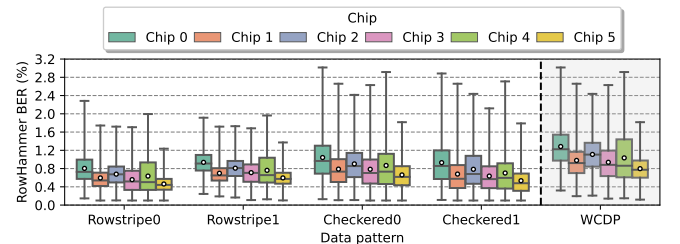


Figure 4:  $BER$  across different HBM2 chips. Error bars show the range of  $BER$  across all tested rows in each chip.

**Obsv. 1.** There are RowHammer bitflips in all tested DRAM rows in all chips.

**Obsv. 2.** RowHammer  $BER$  varies across chips.



For example, Chip 0 has DRAM rows that exhibit up to (on average) 3.02% (1.04%), whereas Chip 5 has rows that exhibit up to (on average) 1.82% (0.66%)  $BER$  for the Checkered 0 data pattern. We observe the most significant difference in chip-level  $BER$  between Chip 0 (1.28%) and Chip 5 (0.80%) as 0.49 for the WCDP.

**Obsv. 3.** *Data patterns affect RowHammer  $BER$ .*

As an example, the Checkered 0 and Checkered 1 data patterns result in substantially higher mean  $BER$  across rows for every DRAM chip compared to the Rowstripe 0 and Rowstripe 1 data patterns. The mean  $BER$  across all tested DRAM rows is 0.76% and 0.67% for Checkered 0/1 and Rowstripe 0/1 data patterns, respectively.

**Takeaway 1.** There are RowHammer bitflips in every tested HBM2 chip. The  $BER$  can reach up to 3.02% (up to 247 bits in a row of 8192 bits).

Figure 5 shows the distribution of  $HC_{first}$  (y-axis) across all tested DRAM rows for each tested data pattern (x-axis). A lower  $HC_{first}$  indicates worse RowHammer vulnerability as DRAM cells exhibit RowHammer bitflips with fewer aggressor row activations (i.e., it takes a shorter time to induce the first RowHammer bitflip in a row).

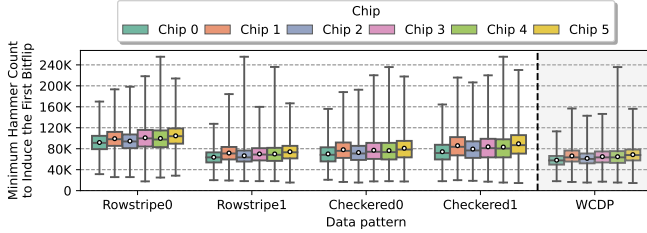


**Figure 5:**  $HC_{first}$  across different DRAM rows, channels, and data patterns

**Obsv. 4.** *It only takes 14531 aggressor row activations to induce a RowHammer bitflip.*

The most RowHammer vulnerable DRAM row across all tested rows has an  $HC_{first}$  of 14531. Causing this bitflip in a row in Chip 5 takes us 1.3 milliseconds.

**Obsv. 5.** *There are rows in every chip that exhibit relatively small  $HC_{first}$  values.*

The other tested chips (Chips 0-4) display similar minimum  $HC_{first}$  values. It takes 18087, 16611, 15500, 17164, and 15500 aggressor row activations to induce the first RowHammer bitflip in Chips 0-4, respectively.

**Obsv. 6.**  *$HC_{first}$  varies across chips.*

There is variation in  $HC_{first}$  distributions between different chips for the same data pattern. For example, the mean  $HC_{first}$  value for Chip 5 is 10.59% higher than the mean  $HC_{first}$  value for Chip 2 using the Rowstripe 0 data pattern.

**Takeaway 2.** HBM2 chips exhibit different levels of RowHammer vulnerability in terms of mean  $BER$  (up to 0.49%) and minimum  $HC_{first}$  (up to 3556).

## 4.2. RowHammer Across Channels

Figure 6 shows the distribution of  $BER$  (y-axis) across different DRAM rows for a given data pattern (x-axis) in a channel (color-coded).

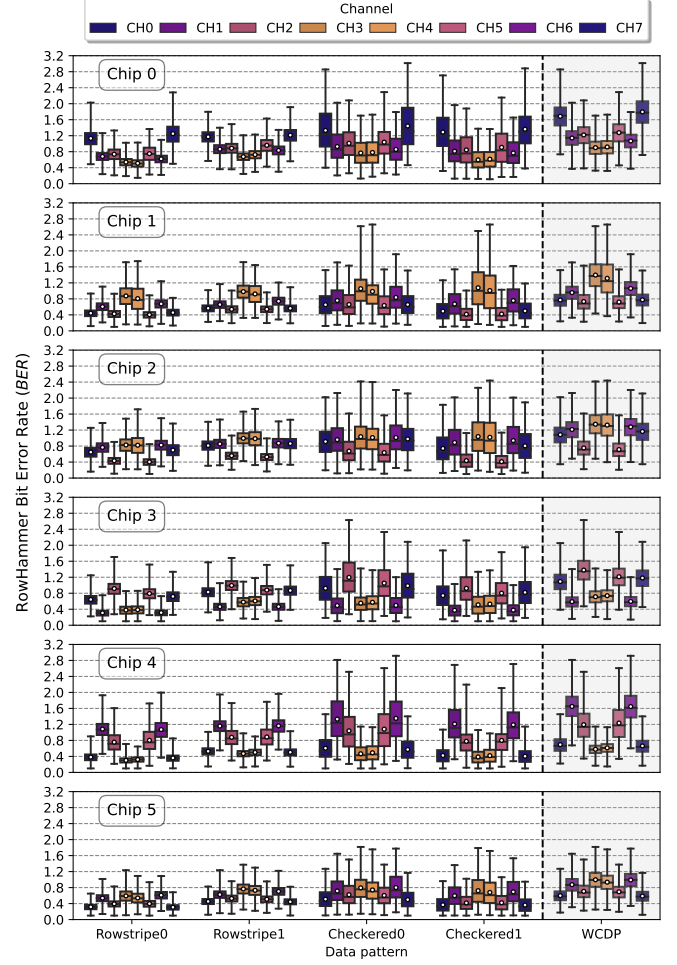


**Figure 6:**  $BER$  across different DRAM rows, channels, and data patterns. Error bars show the range of  $BER$  across rows.

**Obsv. 7.** *There are RowHammer bitflips in each tested DRAM row across all tested HBM2 channels.*

The worst-case data pattern (WCDP)  $BER$  across all tested DRAM rows in all chips can reach 3.02% (i.e., 247 bitflips out of 8192 bits in a row).

**Obsv. 8.**  *$BER$  varies across channels in a chip.*

For example, in Chip 0, channels CH0 and CH7 exhibit significantly higher  $BER$  than other channels. CH7 (where we observe the highest mean  $BER$ ) has  $1.99\times$  the  $BER$  of CH3 (where we observe the lowest mean  $BER$ ) for WCDP. We observe that channels can be classified into groups of two based on the number of bitflips they exhibit. We highlight these groups using different shades of the same color in Figure 6. For example, channels CH3 and CH4 exhibit a similar  $BER$  distribution across rows in every tested HBM2 chip. We hypothesize that groups of channels are spread across different HBM2 DRAM dies. The difference in  $BER$  across the groups of channels could be due to process variation (similar to how

different DDR3/4 chips exhibit different RowHammer characteristics [1, 68, 70, 97, 98].

**Obsv. 9.** *BER distribution across rows in the same channel changes with the data pattern.*

For example, in Chip 0, the maximum observed *BER* in CH7 is 3.02% and 1.91% for data patterns Checkered0 and Rowstripe1, respectively.

**Obsv. 10.** *The distribution of BER across channels changes from chip to chip.*

The most RowHammer vulnerable channel (i.e., a channel with relatively high RowHammer *BER*) is *not* necessarily the same across every chip. For example, channels CH0 and CH7 have the highest average *BER* in Chip 0, whereas channels CH3 and CH4 have the highest average *BER* in Chip 1 for WCDP. We hypothesize that this difference could be due to the effects of process variation across HBM2 chips and HBM2 dies inside chips.

**Obsv. 11.** *BER difference across channels in multiple chips is more prominent than BER difference across all chips.*

For example, the difference between the maximum and the minimum mean *BER* across all rows in each channel in Chip 4 is 0.88%, whereas the difference between the maximum and the minimum mean *BER* across all rows in each chip is 0.38% (see Figure 6), for the Checkered 0 data pattern. This observation holds for all tested data patterns and chips except Chip 5. Chip 5 has a smaller difference between the maximum and the minimum mean *BER* across all rows in each channel than the difference across all rows in each chip.

Figure 7 shows the distribution of  $HC_{first}$  (y-axis) across different DRAM rows for a given data pattern (x-axis) in a channel (color-coded).

**Obsv. 12.** *Different channels exhibit different  $HC_{first}$  distributions.*

For example, channels 3 and 4 in chip 1 contain more rows with smaller  $HC_{first}$  values than other channels. Because these channels also exhibit more RowHammer bitflips than other channels in chip 1 (see Figure 6), we hypothesize that these channels belong in the die with the worst RowHammer vulnerability across all dies.

**Obsv. 13.** *The  $HC_{first}$  distribution in a channel changes with the data pattern.*

For example, the median  $HC_{first}$  for Rowstripe0 and Rowstripe1 in channel 0 in chip 1 are 103905 and 75990, respectively. Testing with different data patterns is necessary to assess the RowHammer vulnerability of an HBM2 DRAM chip, as no data pattern individually achieves the smallest  $HC_{first}$  or the highest *BER* (Figure 6).

**Takeaway 3.** RowHammer *BER* and  $HC_{first}$  significantly vary between different 3D-stacked HBM2 channels in a chip and with the data patterns in aggressor and victim rows. Variation in mean *BER* is larger across channels in multiple chips than the variation in mean *BER* across all chips.

Figure 8 shows the *BER* (y-axis) for each DRAM row (x-

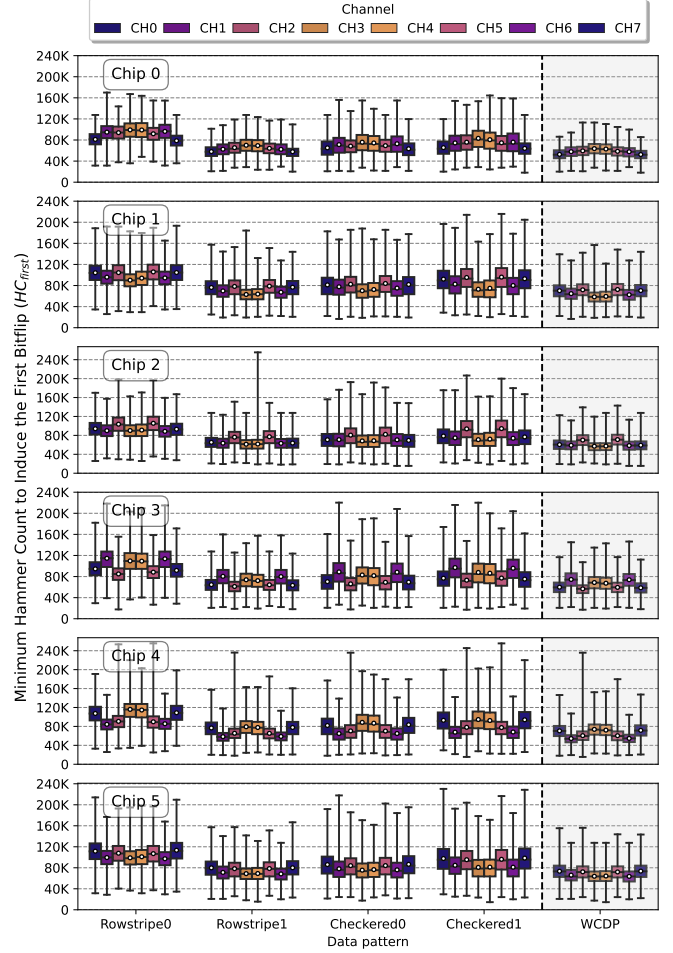


**Figure 7:**  $HC_{first}$  across different DRAM rows, channels, and data patterns.

axis) in a bank when we use the worst-case data pattern (WCDP) to initialize the rows. Each color-coded *BER* curve represents the *BER* for rows in three different channels. The shaded regions indicate variable-sized *subarray* boundaries.<sup>3</sup> For example, the green highlighted subarray (SA X) comprises 832, and the blue highlighted subarray (SA Y) comprises 768 DRAM rows.

**Obsv. 14.** *The BER periodically increases and decreases across DRAM rows.*

This observation is consistent in each tested chip. The *BER* is higher in the middle of a *subarray* and lower towards either end of the subarray. We hypothesize that the increasing and decreasing pattern results from the structure of the local DRAM array. For example, the RowHammer vulnerability of a row could increase with the row's distance from the row buffer.

**Obsv. 15.** *The last and the middle subarray in a bank exhibit relatively low BER.*

<sup>3</sup>We reverse engineer subarray boundaries by performing single-sided RowHammer [1, 68] that induces bitflips in *only one* of the victim rows if the aggressor row is at the edge of a subarray. We find that a subarray contains either 832 (SA X in Figure 8) or 768 (SA Y in Figure 8) DRAM rows.

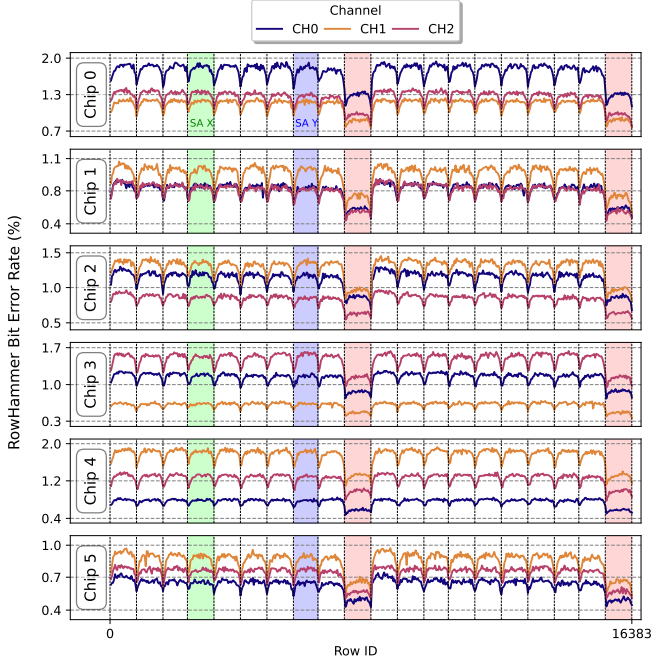


**Figure 8: BER for different rows across a bank in different channels. Highlighted regions show individual DRAM subarrays.**

We observe that the last and the middle subarray in a bank (highlighted with red color in Figure 8), which contain the last and the middle 832 DRAM rows, exhibit significantly lower BER than the other subarrays. We hypothesize that these subarrays exhibit smaller BER due to the micro-architectural characteristics of the DRAM bank. For example, assuming that proximity to the shared I/O circuitry on the DRAM die affects the RowHammer vulnerability of a subarray, the last and the middle subarrays might be placed near this shared I/O circuitry [99].

**Takeaway 4.** A subset of HBM2 rows (the middle and the last 832 rows) are significantly more RowHammer resilient than the other rows in an HBM2 channel.

### 4.3. RowHammer Across Banks and Pseudo Channels

To investigate the variation in the RowHammer vulnerability across HBM2 banks and pseudo channels, we measure BER on 300 rows from 256 banks in chip 0.<sup>4</sup> Figure 9 compares different banks' BER distributions across channels (color) and pseudo channels (marker style) in terms of the coefficient of variation (CV)<sup>5</sup> (x-axis) and mean BER (y-axis). We draw one marker for each bank in the figure. At a high level, a marker close to the y-axis (e.g., the leftmost markers) indicates that the variation in BER across rows in that bank is smaller. A marker close to the x-axis (e.g., the bottommost markers) suggests that the mean BER across rows in that bank is smaller.

<sup>4</sup>First, middle, and last 100 rows in each of the 256 banks spread across eight channels and two pseudo channels.

<sup>5</sup>Coefficient of variation is the standard deviation of a distribution normalized to the mean.

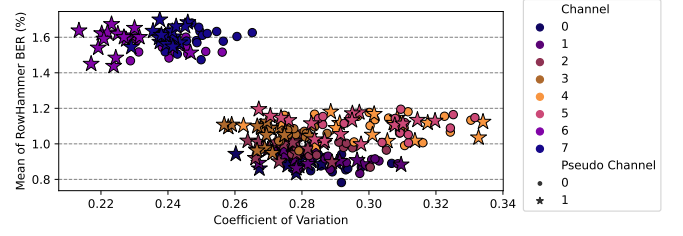


**Figure 9: BER variation across banks. Each bank is represented by the average BER (y-axis) and the coefficient of variation in BER (x-axis) across the rows within the bank.**

**Obsv. 16.** RowHammer BER varies across banks and pseudo channels.

For example, there is up to 0.23 difference in mean BER across banks in channel 7. The markers follow a bimodal distribution (i.e., the markers are clustered around two points in the plot). The two clusters indicate that 1) a bank with a higher mean BER across its rows also has a smaller deviation (i.e., smaller coefficient of variation) from BER across its rows and 2) a bank with a smaller mean BER across its rows also has a larger deviation from BER across its rows.

**Obsv. 17.** The BER variation across banks is dominated by variation across channels.

Banks in different channels tend to have a larger BER difference than banks in the same channel (Figure 6). This indicates that testing different channels is more important than testing different banks or pseudo channels in providing a comprehensive understanding of the RowHammer vulnerability in HBM2 DRAM chips.

**Takeaway 5.** RowHammer BER varies between pseudo channels and banks. This variation is less prominent than the BER variation between channels.

## 5. RowHammer's Sensitivity to Hammer Count

We analyze the number of aggressor row activations needed (hammer count) to induce up to 10 bitflips in a DRAM row. Our  $HC_{first}$  analysis already introduces the hammer count to induce one (*the first*) bitflip in a row. We use the same naming convention used with  $HC_{first}$  to refer to these 9 new hammer counts that we determine in this analysis. For example, we call the hammer count to induce *the second* bitflip  $HC_{second}$  and *the tenth* bitflip  $HC_{tenth}$ . We report the 9 new hammer counts in terms of  $HC_{first}$  where we normalize the new hammer counts to  $HC_{first}$ . For example, if a row's  $HC_{first}$  is 10 and its  $HC_{second}$  normalized to  $HC_{first}$  is 2, the absolute  $HC_{second}$  of the row is 20. We record the hammer counts to induce up to 10 bitflips in 32 rows from each of the beginning, middle, and end of one bank in two channels (that exhibit the smallest  $HC_{first}$  across all channels) in every HBM2 chip.

Figure 10 plots the distribution of all 10 hammer counts (x-axis) normalized to  $HC_{first}$  (y-axis) for all tested DRAM rows (1152 such rows across all chips).

**Obsv. 18.** The normalized hammer count to induce up to 10 bitflips in a row significantly varies between rows.



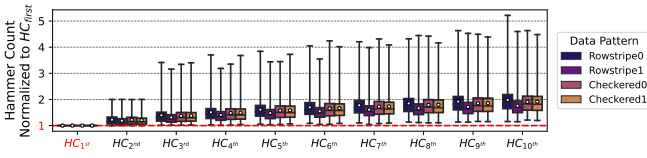


**Figure 10: Distribution of hammer counts (y-axis) to induce up to 10 bitflips in a DRAM row (x-axis), normalized to the row’s  $HC_{first}$ .**

The hammer count to induce up to 10 bitflips in a row can be as small as  $1.15\times$  and as large as  $5.22\times$  the  $HC_{first}$  of the DRAM row. Fewer than  $2\times HC_{first}$  hammers are enough to induce 10 bitflips in a DRAM row on average across all tested DRAM rows. For example, an average DRAM row’s  $HC_{second}$ ,  $HC_{fourth}$ ,  $HC_{eighth}$ , and  $HC_{tenth}$  are  $1.19\times$ ,  $1.41\times$ ,  $1.66\times$ , and  $1.76\times$  that of the row’s  $HC_{first}$  for the Rowstripe 1 data pattern.

**Obsv. 19.** *The hammer counts to induce up to 10 bitflips are moderately affected by data patterns.*

For example, the difference between the largest (Rowstripe0) and the smallest (Rowstripe1) mean normalized  $HC_{tenth}$  is 12.59%. The variation in normalized hammer count across data patterns resembles the variation in  $HC_{first}$  across data patterns (see Figure 5).

Figure 11 plots the additional (over  $HC_{first}$ ) hammer count to induce the  $10^{th}$  bitflip (y-axis) for all tested DRAM rows whose  $HC_{first}$  values are depicted on the x-axis. We compute the additional hammer count for a row as the row’s  $HC_{tenth} - HC_{first}$ . Figure 11 shows one subplot for each of the 6 tested HBM2 chips.

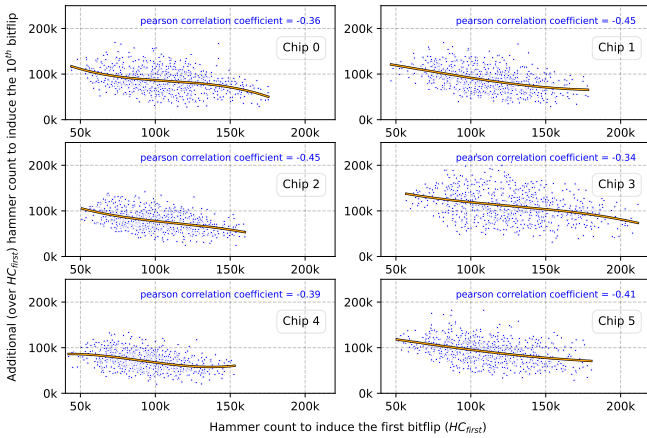


**Figure 11: Additional (over  $HC_{first}$ , x-axis) hammer count needed to induce the  $10^{th}$  bitflip (y-axis) for each tested DRAM row in each tested chip (labeled Chip 0 to Chip 5 in the figure). We plot a polynomial curve fit (orange curve) for each distribution to highlight the decreasing additional hammer count trend with increasing  $HC_{first}$ .**

**Obsv. 20.** *It takes fewer additional hammer counts (over  $HC_{first}$ ) to induce the  $10^{th}$  RowHammer bitflip for a DRAM row with a large  $HC_{first}$  (rows to the right in Figure 11) compared to a DRAM row with a small  $HC_{first}$  (rows to the left in Figure 11).*

We observe that increasing  $HC_{first}$  is correlated with de-

creasing *additional* hammer count to induce the  $10^{th}$  bitflip. We compute the Pearson correlation coefficient for each distribution to quantify the correlation. We conclude that increasing  $HC_{first}$  is *moderately* correlated with decreasing additional hammer count to induce the  $10^{th}$  bitflip, based on the weakest ( $-0.34$ ) and the strongest ( $-0.45$ ) Pearson correlation we observe across distributions for each chip (displayed on each subplot).

**Takeaway 6.** It can take fewer aggressor row activations to induce multiple (e.g., 10) bitflips in a DRAM row if it takes many activations to induce the first bitflip in the row.

## 6. RowHammer and RowPress’s Sensitivities to Aggressor Row On Time

With aggressive technology node scaling, DRAM suffers from worsening read-disturbance effects. One prominent example to read-disturbance in DRAM is RowHammer, which we extensively characterize in our HBM2 chips. We also investigate the characteristics of another widespread read-disturbance effect called RowPress, recently experimentally demonstrated in real DDR4 chips by [4]. RowPress shows that keeping an aggressor row open for a long period of time (i.e., a large aggressor row on time,  $t_{AggON}$ ) induces bitflips in physically nearby DRAM rows with orders of magnitude smaller hammer counts compared to a traditional RowHammer access pattern which keeps the aggressor row open for a short period of time. We provide the first extensive analysis of the RowPress phenomenon in six real HBM2 chips.

Figure 12 depicts how the  $BER$  (y-axis) varies with increasing  $t_{AggON}$  (x-axis) across the first, middle, and last 128 rows in one DRAM bank for 8 channels when we use a hammer count of 150K (i.e., activate and precharge each aggressor row 150K times) and the Checkered 0 data pattern. We plot four relatively small (left subplots) and two relatively large (right subplots)  $t_{AggON}$  values. The minimum  $t_{AggON}$  is determined by the  $t_{RAS}$  timing parameter [74, 76]. We choose two relatively large  $t_{AggON}$  values of interest as  $t_{REFI}$ , the average interval between two successive periodic refresh commands, and as  $9 * t_{REFI}$ , the maximum interval between two subsequent periodic refresh commands (i.e., the maximum time a row can remain open according to the HBM2 standard) [74].<sup>6</sup>

**Obsv. 21.**  *$BER$  in each chip consistently increases with  $t_{AggON}$  in all tested channels.*

<sup>6</sup> $t_{AggON}$  values above 116.0 ns combined with the 150K hammer count results in experiment times that are longer than the 32 ms refresh window, where DRAM cells can exhibit *retention failures*. Because we want to analyze *only* the read disturbance bitflips, we remove bitflips that are caused by retention failures from the set of bitflips we observe at every such  $t_{AggON}$ . To do so, we perform retention profiling experiments where we initialize a tested DRAM row with the Checkered 0 data pattern, wait for the tested retention time to pass (34.8 ms, 1.17 s, and 10.53 s for  $t_{AggON}$  116.0 ns, 3.9  $\mu$ s, and 35.1  $\mu$ s, respectively), and read back the DRAM row. We perform each such experiment 5 times and consider a cell to exhibit retention failures at the tested retention time if the cell exhibits a retention failure in any of the 5 experiments.



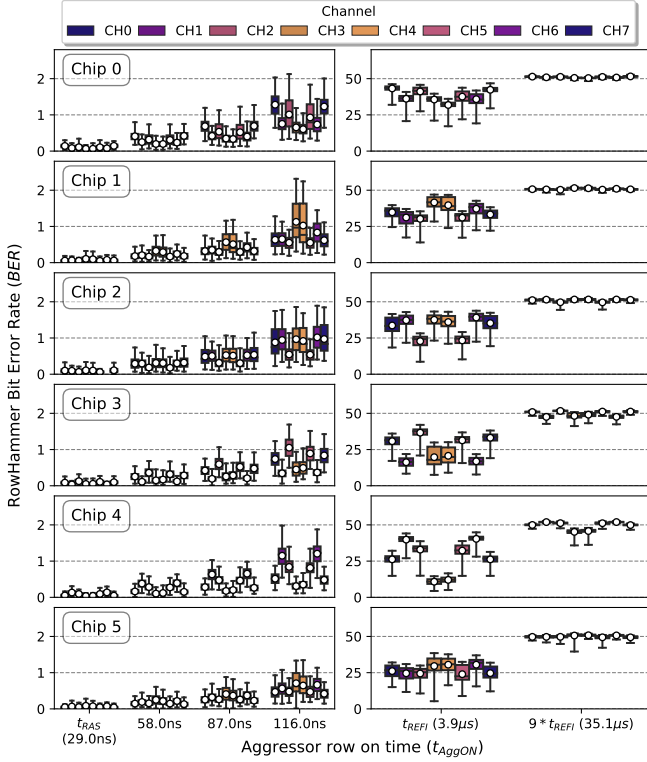


Figure 12: BER with increasing  $t_{AggON}$ .

The average BER across every channel in every chip is 0.08, 0.24, 0.40, 0.73, 31.00, and 50.35 at  $t_{AggON}$  of 29.0 ns, 58.0 ns, 87.0 ns, 116.0 ns, 3.9  $\mu$ s, and 35.1  $\mu$ s, respectively.

**Obsv. 22.** Channels that exhibit higher BER at lower  $t_{AggON}$  values tend to exhibit higher BER also at higher  $t_{AggON}$  values.

For example, Channel 1 in Chip 3 has the highest mean BER across all tested  $t_{AggON}$  values. We observe that all BER values converge to around 50% for the  $t_{AggON}$  of 35.1  $\mu$ s across all tested chips and channels. We hypothesize that this is due to the combined effect of 1) the data pattern that we use which initializes a victim DRAM row with alternating *logic-1* and *logic-0* (i.e., 10101010...) and 2) RowPress causing bitflips from *logic-1* to *logic-0* more frequently than from *logic-0* to *logic-1* (as demonstrated in [4] for a wide variety of DDR4 chips).

Figure 13 depicts how the  $HC_{first}$  values (y-axis) across 384 tested DRAM rows in a channel change with increasing  $t_{AggON}$  (x-axis) for 3 channels when we use the Checkered 0 data pattern. From left to right, 1) the default  $t_{RAS}$  value (29.0 ns), 2)  $t_{REFI}$ , the average time interval between two successive periodic refresh commands, 3)  $9 * t_{REFI}$ , the maximum time a row can remain open according to the HBM2 specification, and 4) half the refresh window ( $t_{REFW}$ ) [74] (such that each aggressor row can be activated once in a  $t_{REFW}$ ). Figure 13 shows one subplot for every tested HBM2 chip. The grey boxes indicate the number of rows we show in each subplot. We only show rows for which we observe the first read-disturb bitflip in a refresh window (under 32 ms) at every tested  $t_{AggON}$  value. We display the results for four  $t_{AggON}$  values on the x-axis.

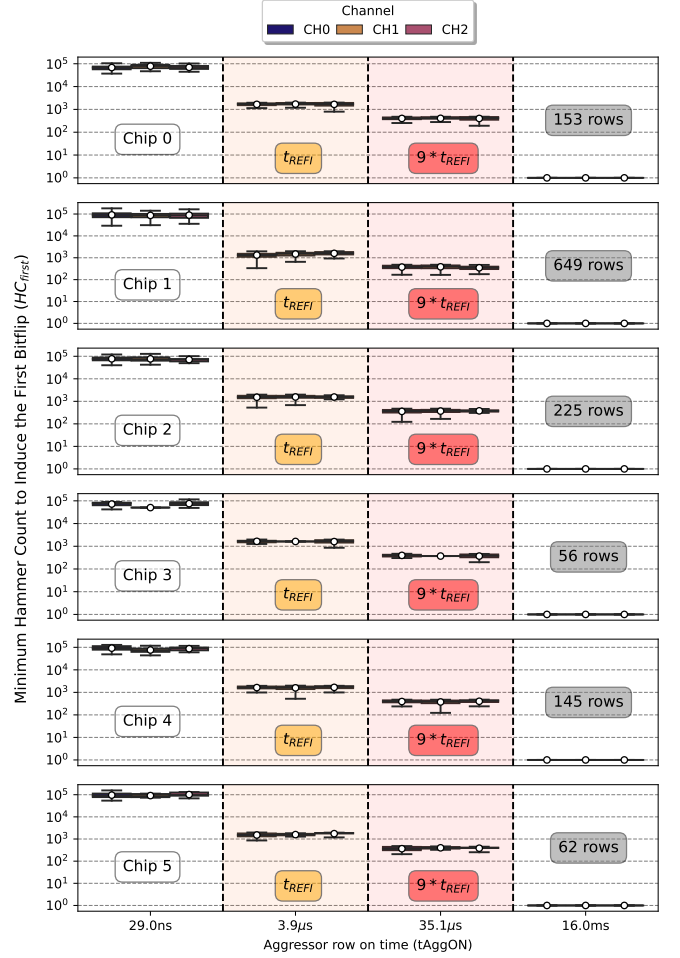


Figure 13:  $HC_{first}$  with increasing  $t_{AggON}$ .

**Obsv. 23.** As the aggressor row remains open longer (i.e., as  $t_{AggON}$  increases), DRAM rows experience bitflips with fewer hammer counts.

This observation is consistent across the three tested HBM2 channels. The average (minimum)  $HC_{first}$  values across all chips are 83689 (29183), 1519 (335), 376 (123), and 1 (1), for the four tested  $t_{AggON}$  values, respectively.

**Takeaway 7.** The read-disturbance vulnerability of tested HBM2 chips worsens (i.e., BER increases and  $HC_{first}$  reduces) with increasing  $t_{AggON}$ .

Our observations are in line with prior work that investigate the effects of aggressor row on time in real DDR4 chips [4, 70].

## 7. In-DRAM RowHammer Defenses

To prevent RowHammer bitflips, DRAM manufacturers equip their chips with a mitigation mechanism broadly referred to as Target Row Refresh (TRR) [38, 44, 75]. Proprietary versions of TRR (e.g., in DDR4) operate transparently from the perspective of the memory controller. At a high level, TRR identifies potential aggressor rows as the memory controller issues activate commands to the DRAM chip and TRR preventively refreshes their victim rows when the memory controller issues a periodic

*REF* command. Contrary to the proprietary TRR mechanisms implemented in DDR4, HBM2 implements the TRR Mode and describes its operation in the standard specification [74].

We demonstrate that a tested HBM2 chip (Chip 0 in Table 3) implements a form of proprietary TRR (similar to the ones used in DDR4) on top of the TRR Mode defined in the HBM2 standard. We analyze the TRR mechanism and craft a specialized attack pattern that bypasses the TRR mechanism and induces RowHammer bitflips.

**Methodology.** We use U-TRR’s [44] methodology to uncover the proprietary TRR mechanism. The key idea of this methodology is to use retention failures as a side channel to infer whether or not TRR refreshes a DRAM row.

Our analysis consists of two steps. First, we identify multiple DRAM rows with similar retention times (e.g., two rows that can correctly retain data when they are not refreshed for the same amount of time) by profiling DRAM rows for their retention times. We test all of the DRAM rows in bank 0 for retention failures starting with a retention time of 64 ms with increments of 64 ms. We deem a row to have a retention time of T if any of the DRAM cells in the row exhibit a bitflip at a retention time of T.

Second, to understand if the TRR mechanism samples an aggressor row, we execute a four-step process: 1) We initialize DRAM rows that have a retention time of T (we call these rows *side-channel rows*) and wait for T/2 *without* refreshing these rows. 2) We activate each of the DRAM rows adjacent to the side-channel rows *once*. We hypothesize that the TRR mechanism samples an activation to an adjacent row as an aggressor row activation. 3) We issue a *REF* command to trigger the TRR mechanism. If the TRR mechanism had sampled any of the activated adjacent rows in step 2, we expect the TRR mechanism to refresh the side-channel rows. 4) We wait for T/2, read the data in the side-channel rows and check for any retention bitflips. The side-channel rows exhibit retention bitflips *only* if they are not refreshed by the TRR mechanism. We use this information to understand how the TRR mechanism works.

We repeat our experiment with various carefully crafted RowHammer access patterns to understand how the TRR mechanism tracks the aggressor rows.

**Obsv. 24.** Every 17<sup>th</sup> *REF* command can perform a TRR victim row refresh (i.e., every 17<sup>th</sup> *REF* command is TRR-capable).

This resembles the TRR mechanism employed in real DDR4 chips from Vendor C in U-TRR [44].

**Obsv. 25.** The TRR mechanism refreshes both of the adjacent rows of an aggressor row it detects.

If TRR detects row R as an aggressor row, it refreshes rows R+1 and R-1.

**Obsv. 26.** The first row that gets activated after a TRR-capable *REF* is always detected as an aggressor row by the TRR mechanism.

**Obsv. 27.** The TRR mechanism records the activation count of activated rows and uses this record to detect if a row is an aggressor row.

Between two *REF* commands, if a row is activated more than half the total activation count, the TRR mechanism detects that row as an aggressor row. For example, if we issue 10 activations between two *REF* commands, the row that receives the first *ACT* command and the row that receives 5 *ACT* commands are detected by the TRR mechanism.

**Takeaway 8.** An HBM2 chip implements a proprietary TRR mechanism that tracks aggressor rows and proactively refreshes their victim rows.

**Bypassing the proprietary TRR mechanism.** Based on our observations, we craft a specialized attack pattern that bypasses the TRR mechanism and causes RowHammer bitflips. We calculate the total activation budget (i.e., the maximum number of *ACT* commands that the memory controller can issue) between two *REF* commands as  $\lfloor (t_{REFI} - t_{RFC}) / t_{RC} \rfloor = 78$  [74, 76] for the tested HBM2 chip and fully utilize the activation budget in our attack pattern. The key idea of this attack pattern is to trick TRR into *not* detecting a *real* aggressor row by repeatedly accessing multiple *dummy* rows many times. The attack pattern 1) activates dummy rows (we vary the number of dummy rows and the activation count of the dummy rows) and 2) performs a double-sided RowHammer attack using two real aggressor rows. We create this attack pattern such that the number of real aggressor activations does not exceed half of the total activation budget. We repeat the attack pattern  $8205 * 2$  times (i.e., approximately for two  $t_{REFW}$ , 64 ms) for each DRAM row in a bank so that we activate aggressor rows as many times as possible before each DRAM cell is refreshed at least once.

We test all rows in a bank of the HBM2 chip using this attack pattern while obeying manufacturer-recommended timing parameters (e.g., we issue a *REF* command every  $t_{REFI}$ , 3.9  $\mu$ s). Figure 14 shows the distribution of the RowHammer bit error rate for different numbers of dummy rows (x-axis) and aggressor activation counts (different boxes). Since we have a total activation budget of 78 and we utilize the whole budget for aggressor row and dummy row activations, the number of dummy row activations varies between boxes displayed on the plot. For example, for 4 dummy rows and an aggressor activation count of 18 (leftmost box in Figure 14), each dummy row is activated  $\lfloor (78 - 18 * 2) / 4 \rfloor = 10$  times.

We make three key observations from Fig. 14. First, the attack pattern needs to activate at least 4 dummy rows to bypass the TRR mechanism. Second, the number of dummy rows does *not* significantly affect the distribution of the bit error rate. For example, the mean bit error rate varies by 0.003 between the largest (4 dummy rows) and the smallest (7 dummy rows) value at an aggressor activation count of 34. Third, the number of bitflips per row increases as the aggressor activation count increases. For example, the mean bit error rate increases by  $2.79\times$ ,  $6.72\times$ , and  $10.28\times$  as the aggressor activation count increases from 18 to 24, 30, and 34, respectively, when the number of dummy rows is 8.

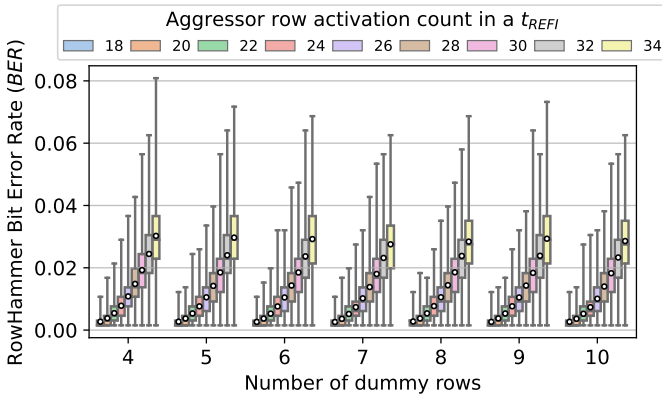


**Figure 14: RowHammer bit error rate (y-axis) distribution across all tested DRAM rows when we execute the specialized attack pattern with different number of dummy rows (x-axis) and different aggressor row activation counts (different colored boxes).**

**Takeaway 9.** A specialized attack pattern that bypasses the undocumented TRR mechanism in HBM2 chips can induce many RowHammer bitflips.

## 8. Implications on Future Read Disturbance Attacks and Defenses

We describe and analyze the important implications of our observations (Section 4, Section 5, Section 6, and Section 7) on future read disturbance attacks and defenses.

### 8.1. Read Disturbance Attacks

Takeaways 1, 3, 7, and 8 have the following 4 implications for future read disturbance attacks on HBM2 chips. First, the maximum *BER* (247 bitflips in a row of 8192 bits) we observe across tested chips exceeds the correction capabilities of widely used error correcting codes (ECC), such as SECDED [100, 101] which can detect two bitflips and correct one bitflip in a code-word (Takeaway 1). 247 bitflips in a row are already sufficient to induce uncorrectable bitflips in multiple 64-bit words in the same DRAM row (by pigeonhole principle) and are likely to induce undetectable bitflips in at least one 64-bit word. To give a concrete example, we investigate the distribution of word-level RowHammer bitflips (i.e., bitflips that occur in all non-overlapping consecutive 64 bits) in Chip 4. Figure 15 plots the number of words with at least one bitflip (out of all 18M tested words) on the y-axis over the different maximum number of bitflips in a word depicted on the x-axis for different data patterns (different bars). The word counts across clusters of bars are non-overlapping; for example, the middle cluster depicts the number of words with exactly two bitflips.

We make two observations. First, the number of unique words with more than two bitflips is substantially large. We observe 974’935 words with more than two bitflips when we use the Checkered0 data pattern. These bitflips would *not* be detected by SECDED ECC. Second, most words with at least one bitflip actually have more than one bitflips. In other words, if RowHammer bitflips can be induced in a word, it is very

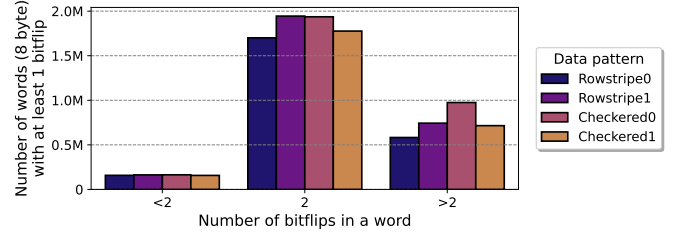


**Figure 15: Number of words (y-axis) with different number of bitflips (x-axis) in Chip 4.**

likely that there will be more than one bit location in the word that will experience errors. SECDED ECC *cannot* correct such bitflips.

We find that an HBM word can have 16 bitflips (not shown in the figure) in Chip 4. A (7,4) Hamming code [102] could correct such bitflips at very large (75%, 3 parity bits for every 4 data bits) DRAM storage overheads. Thus, relying on ECC alone to prevent RowHammer bitflips in HBM2 is a very expensive solution. The bitflip distributions indicate that attackers could exploit RowHammer bitflips to escalate privilege and leak security-critical and secret data in HBM2 chips, as demonstrated by real RowHammer attacks on DDR4-based computing systems. Even if an HBM2 chip is highly RowHammer resilient (i.e., has small mean *BER* across its rows), malicious parties could exploit RowHammer bitflips to practically increase the rate of correctable or detectable bitflips. This could reduce the lifetime of modern HBM-based systems (e.g., GPUs) by accelerating the rate of memory page retirements beyond design-time estimates and exacerbate system maintenance costs [103].

Second, a RowHammer attack could target the most-RowHammer-vulnerable HBM2 channel to reduce the time it spends on i) *preparing* for an attack, by finding exploitable RowHammer bitflips faster (i.e., by accelerating memory templating), and ii) *performing* the attack, by benefitting from a small  $HC_{first}$  value (Takeaway 3). Third, an attacker could keep the aggressor row on for longer by executing specialized access patterns (as demonstrated by RowPress in a real DDR4-based system [4]) to benefit from the increased *BER* and reduced  $HC_{first}$  when aggressor HBM2 rows are kept open for longer (Takeaway 7). Fourth, the RowHammer attack must uncover and take into account the functionality of the undocumented TRR mechanism in addition to the functionality of the documented TRR mode [74] to come up with an effective access pattern that bypasses all RowHammer defense mechanisms in an HBM2-based system (Takeaway 8). However, the attackers can also benefit from the undocumented TRR mechanism. The victim row refreshes performed by the TRR mechanism could be used as a near aggressor row activation, carrying over the read disturbance effects of the far aggressor row to the victim row in a HalfDouble access pattern [47].

### 8.2. Read Disturbance Defenses

Takeaways 3, 4, and 9 have the following 2 implications for future read disturbance attacks on HBM2 chips.

First, a RowHammer defense mechanism can adapt to the heterogeneous distribution of the RowHammer and RowPress vulnerability across channels and subarrays, which may allow the defense mechanism to more efficiently prevent read disturbance bitflips (Takeaways 3 and 4). Second, HBM2 memory controller designers likely need to implement other read disturbance defense mechanisms (e.g., [1, 3, 24, 31, 38, 44, 95, 104–133, 133–164]) in their designs because designers cannot rely on the undocumented TRR mechanism to mitigate read disturbance bitflips as this mechanism can be easily bypassed with carefully crafted RowHammer access patterns (Takeaway 9).

## 9. Related Work

We present the first detailed experimental characterization of the read disturbance vulnerability (RowHammer and RowPress) in six modern HBM2 DRAM chips.

**HBM2 RowHammer Characterization [165].** A prior work experimentally characterizes the RowHammer vulnerability in an HBM2 DRAM chip. Our work presents a detailed experimental characterization of both RowHammer and RowPress using multiple HBM2 chips. In addition to analyzing the spatial variation of both RowHammer and RowPress vulnerabilities, we analyze the hammer counts needed to induce the first 10 bitflips in a row. We uncover entirely the inner workings of the in-DRAM read disturbance defense mechanisms in an HBM2 chip and demonstrate RowHammer access patterns that bypass this defense mechanism. Our new analyses and results lead to completely new observations (Observation 2, 6, 10, 11, 15, 18–27) and takeaways (Takeaway 2, 3, 6–9) that [165] does *not* contain.

**DDR3/4 Read Disturbance Characterization [1, 4, 68–70, 97, 98, 166–169].** These works experimentally demonstrate and analyze new aspects of the read disturbance vulnerability by testing real DDR3/4 DRAM chips. These works do not experimentally analyze real HBM2 chips.

Besides demonstrating the interaction between the read disturbance vulnerability of an HBM2 chip with unique HBM characteristics (e.g., the spatial distribution of the vulnerability across 3D-stacked channels) for the first time, we make new observations (Observation 14, 15, 18, 19, 20) that could also shed light into the read disturbance vulnerability behavior in (LP)DDR chips. For example, our observation of the RowHammer bit error rate peaking towards the middle of a subarray (Observation 14) could be widely spread across many different types of DRAM chips. These observations are *not* made, and the studies that led to such observations are *not* done in prior work. Section 8 highlights the importance of our new observations in the form of several key implications for future RowHammer attacks and defenses.

**Other HBM2 Characterization [170–172].** These works characterize real HBM2 chips to understand their 1) soft error resilience characteristics by high-energy neutron beam testing [172], 2) performance and reliability characteristics under reduced supply voltage [170], and 3) data retention characteristics [171].

## 10. Conclusion

In this work, we presented the results of our detailed characterization study on the read disturbance (RowHammer and RowPress) vulnerability in six modern HBM2 chips. We show that 1) the read disturbance vulnerability is heterogeneously distributed across various components in the HBM2 chip, 2) a DRAM row with a large hammer count to induce the first bitflip requires a smaller additional hammer count to exhibit more bitflips, and 3) read disturbance bitflips can be induced with a hammer count of *only one* if the aggressor row is kept open for a very long time. We discover that the HBM2 chip implements a proprietary read disturbance mitigation mechanism. We uncover the inner workings of this mechanism and develop a practical access pattern that bypasses it and induces read disturbance bitflips. Our new observations have important implications for future read disturbance attacks and defenses: our key takeaways can be leveraged to develop more powerful read disturbance attacks and more efficient read disturbance defenses.

## Acknowledgments

We thank the anonymous reviewers of DSN Disrupt 2023. We thank the SAFARI Research Group members for feedback and the stimulating intellectual environment. We acknowledge the generous gift funding provided by our industrial partners (especially Google, Huawei, Intel, Microsoft, VMware), which has been instrumental in enabling our decade-long research on read disturbance in DRAM and memory systems. This work was in part supported by a Google Security and Privacy Research Award and the Microsoft Swiss Joint Research Center.

## References

- [1] Y. Kim, R. Daly, J. Kim, C. Fallin, J. H. Lee, D. Lee, C. Wilkerson, K. Lai, and O. Mutlu, “Flipping Bits in Memory Without Accessing Them: An Experimental Study of DRAM Disturbance Errors,” in *ISCA*, 2014.
- [2] O. Mutlu and J. Kim, “RowHammer: A Retrospective,” *IEEE TCAD Special Issue on Top Picks in Hardware and Embedded Security*, 2019.
- [3] O. Mutlu, A. Olgun, and A. G. Yaglikci, “Fundamentally Understanding and Solving RowHammer,” in *ASP-DAC*, 2023.
- [4] H. Luo, A. Olgun, A. G. Yaglikci, Y. C. Tuğrul, S. Rhyner, M. B. Cavlak, J. Lindegger, M. Sadrosadati, and O. Mutlu, “RowPress: Amplifying Read Disturbance in Modern DRAM Chips,” in *ISCA*, 2023.
- [5] A. P. Fournaris, L. Pocero Fraile, and O. Koufopavlou, “Exploiting Hardware Vulnerabilities to Attack Embedded System Devices: A Survey of Potent Microarchitectural Attacks,” *Electronics*, 2017.
- [6] D. Poddebniak, J. Somorovsky, S. Schinzel, M. Lochter, and P. Rösler, “Attacking Deterministic Signature Schemes using Fault Attacks,” in *EuroS&P*, 2018.
- [7] A. Tatar, R. K. Konoth, E. Athanasopoulos, C. Giuffrida, H. Bos, and K. Razavi, “Throwhammer: Rowhammer Attacks Over the Network and Defenses,” in *USENIX ATC*, 2018.
- [8] S. Carre, M. Desjardins, A. Facon, and S. Guilley, “OpenSSL Bellcore’s Protection Helps Fault Attack,” in *DSD*, 2018.
- [9] A. Barenghi, L. Breveglieri, N. Izzo, and G. Pelosi, “Software-only Reverse Engineering of Physical DRAM Mappings for Rowhammer Attacks,” in *IVSW*, 2018.
- [10] Z. Zhang, Z. Zhan, D. Balasubramanian, X. Koutsoukos, and G. Karsai, “Triggering Rowhammer Hardware Faults on ARM: A Revisit,” in *ASHES*, 2018.
- [11] S. Bhattacharya and D. Mukhopadhyay, “Advanced Fault Attacks in Software: Exploiting the Rowhammer Bug,” in *Fault Tolerant Architectures for Cryptography and Hardware Security*, 2018.
- [12] M. Seaborn and T. Dullien, “Exploiting the DRAM Rowhammer Bug to Gain Kernel Privileges,” <http://googleprojectzero.blogspot.com.tr/2015/03/exploiting-dram-rowhammer-bug-to-gain.html>, 2015.
- [13] SAFARI Research Group, “RowHammer — GitHub Repository,” <https://github.com/CMU-SAFARI/rowhammer>, 2014.
- [14] M. Seaborn and T. Dullien, “Exploiting the DRAM Rowhammer Bug to Gain Kernel Privileges,” *Black Hat*, 2015.



- [15] V. van der Veen, Y. Fratanio, M. Lindorfer, D. Gruss, C. Maurice, G. Vigna, H. Bos, K. Razavi, and C. Giuffrida, "Drammer: Deterministic Rowhammer Attacks on Mobile Platforms," in *CCS*, 2016.
- [16] D. Gruss, C. Maurice, and S. Mangard, "Rowhammer.js: A Remote Software-Induced Fault Attack in Javascript," in *DIMVA*, 2016.
- [17] K. Razavi, B. Gras, E. Bosman, B. Preneel, C. Giuffrida, and H. Bos, "Flip Feng Shui: Hammering a Needle in the Software Stack," in *USENIX Security*, 2016.
- [18] P. Pessl, D. Gruss, C. Maurice, M. Schwarz, and S. Mangard, "DRAMA: Exploiting DRAM Addressing for Cross-CPU Attacks," in *USENIX Security*, 2016.
- [19] Y. Xiao, X. Zhang, Y. Zhang, and R. Teodorescu, "One Bit Flips, One Cloud Flops: Cross-VM Row Hammer Attacks and Privilege Escalation," in *USENIX Security*, 2016.
- [20] E. Bosman, K. Razavi, H. Bos, and C. Giuffrida, "Dedup Est Machina: Memory Deduplication as An Advanced Exploitation Vector," in *S&P*, 2016.
- [21] S. Bhattacharya and D. Mukhopadhyay, "Curious Case of RowHammer: Flipping Secret Exponent Bits using Timing Analysis," in *CHES*, 2016.
- [22] W. Burleson, O. Mutlu, and M. Tiwari, "Invited: Who is the Major Threat to Tomorrow's Security? You, the Hardware Designer," in *DAC*, 2016.
- [23] R. Qiao *et al.*, "A New Approach for RowHammer Attacks," in *HOST*, 2016.
- [24] F. Brasser, L. Davi, D. Gens, C. Liebchen, and A.-R. Sadeghi, "Can't Touch This: Software-Only Mitigation Against Rowhammer Attacks Targeting Kernel Memory," in *USENIX Security*, 2017.
- [25] Y. Jang, J. Lee, S. Lee, and T. Kim, "SGX-Bomb: Locking Down the Processor via Rowhammer Attack," in *SysTEX*, 2017.
- [26] M. T. Aga, Z. B. Aweke, and T. Austin, "When Good Protections Go Bad: Exploiting Anti-DOS Measures to Accelerate Rowhammer Attacks," in *HOST*, 2017.
- [27] O. Mutlu, "The RowHammer Problem and Other Issues We May Face as Memory Becomes Denser," in *DATE*, 2017.
- [28] A. Tatar, C. Giuffrida, H. Bos, and K. Razavi, "Defeating Software Mitigations Against Rowhammer: A Surgical Precision Hammer," in *RAID*, 2018.
- [29] D. Gruss, M. Lipp, M. Schwarz, D. Genkin, J. Juffinger, S. O'Connell, W. Schoecl, and Y. Yarom, "Another Flip in the Wall of Rowhammer Defenses," in *S&P*, 2018.
- [30] M. Lipp, M. T. Aga, M. Schwarz, D. Gruss, C. Maurice, L. Raab, and L. Lamster, "Nethammer: Inducing Rowhammer Faults Through Network Requests," arXiv:1805.04956, 2018.
- [31] V. van der Veen, M. Lindorfer, Y. Fratanio, H. P. Pillai, G. Vigna, C. Kruegel, H. Bos, and K. Razavi, "GuardION: Practical Mitigation of DMA-Based Rowhammer Attacks on ARM," in *DIMVA*, 2018.
- [32] P. Frigo, C. Giuffrida, H. Bos, and K. Razavi, "Grand Pwning Unit: Accelerating Microarchitectural Attacks with the GPU," in *S&P*, 2018.
- [33] L. Cojocar, K. Razavi, C. Giuffrida, and H. Bos, "Exploiting Correcting Codes: On the Effectiveness of ECC Memory Against Rowhammer Attacks," in *S&P*, 2019.
- [34] S. Ji, Y. Ko, S. Oh, and J. Kim, "Pinpoint Rowhammer: Suppressing Unwanted Bit Flips on Rowhammer Attacks," in *ASIACCS*, 2019.
- [35] O. Mutlu, "RowHammer and Beyond," in *COSADE*, 2019.
- [36] S. Hong, P. Frigo, Y. Kaya, C. Giuffrida, and T. Dumitras, "Terminal Brain Damage: Exposing the Graceless Degradation in Deep Neural Networks Under Hardware Fault Attacks," in *USENIX Security*, 2019.
- [37] A. Kwong, D. Genkin, D. Gruss, and Y. Yarom, "RAMBleed: Reading Bits in Memory Without Accessing Them," in *S&P*, 2020.
- [38] P. Frigo, E. Vannacci, H. Hassan, V. van der Veen, O. Mutlu, C. Giuffrida, H. Bos, and K. Razavi, "TRRespass: Exploiting the Many Sides of Target Row Refresh," in *S&P*, 2020.
- [39] L. Cojocar, J. Kim, M. Patel, L. Tsai, S. Saroiu, A. Wolman, and O. Mutlu, "Are We Susceptible to Rowhammer? An End-to-End Methodology for Cloud Providers," in *S&P*, 2020.
- [40] Z. Weissman, T. Tiemann, D. Moghimi, E. Custodio, T. Eisenbarth, and B. Sunar, "JackHammer: Efficient Rowhammer on Heterogeneous FPGA-CPU Platforms," arXiv:1912.11523, 2020.
- [41] Z. Zhang, Y. Cheng, D. Liu, S. Nepal, Z. Wang, and Y. Yarom, "PTHammer: Cross-User-Kernel-Boundary Rowhammer Through Implicit Accesses," in *MICRO*, 2020.
- [42] F. Yao, A. S. Rakin, and D. Fan, "Deephammer: Depleting the Intelligence of Deep Neural Networks Through Targeted Chain of Bit Flips," in *USENIX Security*, 2020.
- [43] F. de Ridder, P. Frigo, E. Vannacci, H. Bos, C. Giuffrida, and K. Razavi, "SMASH: Synchronized Many-Sided Rowhammer Attacks from JavaScript," in *USENIX Security*, 2021.
- [44] H. Hassan, Y. C. Tugrul, J. S. Kim, V. van der Veen, K. Razavi, and O. Mutlu, "Uncovering In-DRAM RowHammer Protection Mechanisms: A New Methodology, Custom RowHammer Patterns, and Implications," in *MICRO*, 2021.
- [45] P. Jattke, V. van der Veen, P. Frigo, S. Gunter, and K. Razavi, "Blacksmith: Scalable Rowhammering in the Frequency Domain," in *S&P*, 2022.
- [46] M. C. Tol, S. Islam, B. Sunar, and Z. Zhang, "Toward Realistic Backdoor Injection Attacks on DNNs using RowHammer," arXiv:2110.07683, 2022.
- [47] A. Kogler, J. Juffinger, S. Qazi, Y. Kim, M. Lipp, N. Boichat, E. Shiu, M. Nissler, and D. Gruss, "Half-Double: Hammering From the Next Row Over," in *USENIX Security*, 2022.
- [48] L. Orosa, U. Rührmair, A. G. Yaglikci, H. Luo, A. Olgun, P. Jattke, M. Patel, J. Kim, K. Razavi, and O. Mutlu, "SpyHammer: Using RowHammer to Remotely Spy on Temperature," arXiv:2210.04084, 2022.
- [49] Z. Zhang, W. He, Y. Cheng, W. Wang, Y. Gao, D. Liu, K. Li, S. Nepal, A. Fu, and Y. Zou, "Implicit Hammer: Cross-Privilege-Boundary Rowhammer through Implicit Accesses," *IEEE TDSC*, 2022.
- [50] L. Liu, Y. Guo, Y. Cheng, Y. Zhang, and J. Yang, "Generating Robust DNN with Resistance to Bit-Flip based Adversarial Weight Attack," *IEEE TC*, 2022.
- [51] Y. Cohen, K. S. Tharayil, A. Haelen, D. Genkin, A. D. Keromytis, Y. Oren, and Y. Yarom, "HammerScope: Observing DRAM Power Consumption Using Rowhammer," in *CCS*, 2022.
- [52] M. Zheng, Q. Lou, and L. Jiang, "TrojViT: Trojan Insertion in Vision Transformers," arXiv:2208.13049, 2022.
- [53] M. Fahr Jr, H. Kippen, A. Kwong, T. Dang, J. Lichtinger, D. Dachman-Soled, D. Genkin, A. Nelson, R. Perlner, A. Yerukhimovich *et al.*, "When Frodo Flips: End-to-End Key Recovery on FrodoKEM via Rowhammer," *CCS*, 2022.
- [54] Y. Tobah, A. Kwong, I. Kang, D. Genkin, and K. G. Shin, "SpecHammer: Combining Spectre and Rowhammer for New Speculative Attacks," in *S&P*, 2022.
- [55] A. S. Rakin, M. H. I. Chowdhury, F. Yao, and D. Fan, "DeepSteal: Advanced Model Extractions Leveraging Efficient Weight Stealing in Memories," in *S&P*, 2022.
- [56] H. Aydin and A. Serbas, "Cyber Security in Industrial Control Systems (ICS): A Survey of RowHammer Vulnerability," *Applied Computer Science*, 2022.
- [57] K. Mus, Y. Doröz, M. C. Tol, K. Rahman, and B. Sunar, "Jolt: Recovering TLS Signing Keys via Rowhammer Faults," *Cryptology ePrint Archive*, 2022.
- [58] J. Wang, H. Xu, C. Xiao, L. Zhang, and Y. Zheng, "Research and Implementation of Rowhammer Attack Method based on Domestic NeoKylin Operating System," in *ICFTIC*, 2022.
- [59] S. Lefforge, "Reverse Engineering Post-Quantum Cryptography Schemes to Find Rowhammer Exploits," Bachelor's Thesis, University of Arkansas, 2023.
- [60] M. J. Fahr, "The Effects of Side-Channel Attacks on Post-Quantum Cryptography: Influencing FrodoKEM Key Generation Using the Rowhammer Exploit," Master's thesis, University of Arkansas, 2022.
- [61] A. Kaur, P. Srivastav, and B. Ghoshal, "Work-in-Progress: DRAM-MaUT: DRAM Address Mapping Unveiling Tool for ARM Devices," in *CASES*, 2022.
- [62] K. Cai, Z. Zhang, and F. Yao, "On the Feasibility of Training-time Trojan Attacks through Hardware-based Faults in Memory," in *HOST*, 2022.
- [63] D. Li, D. Liu, Y. Ren, Z. Wang, Y. Sun, Z. Guan, Q. Wu, and J. Liu, "CyberRadar: A PUF-based Detecting and Mapping Framework for Physical Devices," arXiv:2201.07597, 2022.
- [64] A. Roohi and S. Angizi, "Efficient Targeted Bit-Flip Attack Against the Local Binary Pattern Network," in *HOST*, 2022.
- [65] F. Staudigl, H. Al Indari, D. Schön, D. Sisejkovic, F. Merchant, J. M. Joseph, V. Rana, S. Menzel, and R. Leupers, "NeuroHammer: Inducing Bit-Flips in Memristive Crossbar Memories," in *DATE*, 2022.
- [66] L.-H. Yang, S.-S. Huang, T.-L. Cheng, Y.-C. Kuo, and J.-J. Kuo, "Socially-Aware Collaborative Defense System against Bit-Flip Attack in Social Internet of Things and Its Online Assignment Optimization," in *ICCCN*, 2022.
- [67] S. Islam, K. Mus, R. Singh, P. Schaumont, and B. Sunar, "Signature Correction Attack on Dilithium Signature Scheme," in *Euro S&P*, 2022.
- [68] J. S. Kim, M. Patel, A. G. Yaglikci, H. Hassan, R. Azizi, L. Orosa, and O. Mutlu, "Revisiting RowHammer: An Experimental Analysis of Modern Devices and Mitigation Techniques," in *ISCA*, 2020.
- [69] A. G. Yaglikci, H. Luo, G. F. De Oliveira, A. Olgun, M. Patel, J. Park, H. Hassan, J. S. Kim, L. Orosa, and O. Mutlu, "Understanding RowHammer Under Reduced Wordline Voltage: An Experimental Study Using Real DRAM Devices," in *DSN*, 2022.
- [70] L. Orosa, A. G. Yaglikci, H. Luo, A. Olgun, J. Park, H. Hassan, M. Patel, J. S. Kim, and O. Mutlu, "A Deeper Look into RowHammer's Sensitivities: Experimental Analysis of Real DRAM Chips and Implications on Future Attacks and Defenses," in *MICRO*, 2021.
- [71] O. Mutlu, "RowHammer," <https://people.inf.ethz.ch/omutlu/pub/onur-Rowhammer-TopPicksinHardwareEmbeddedSecurity-November-8-2018.pdf>, 2018, Top Picks in Hardware and Embedded Security.
- [72] A. Bakhoda, G. L. Yuan, W. W. L. Fung, H. Wong, and T. M. Aamodt, "Analyzing CUDA Workloads Using a Detailed GPU Simulator," in *ISPASS*, 2009.
- [73] S. Che, M. Boyer, J. Meng, D. Tarjan, J. W. Sheaffer, S.-H. Lee, and K. Skadron, "Rodinia: A Benchmark Suite for Heterogeneous Computing," in *IISWC*, 2009.
- [74] JEDEC, *JESD235D: High Bandwidth Memory DRAM (HBM1, HBM2)*, 2021.
- [75] Micron, *16Gb: x4, x8, x16 DDR4 SDRAM Features - MT40A4G4, MT40A2G8, MT40A1G16*, 2018.
- [76] J. M. O'Connor, "Energy Efficient High Bandwidth DRAM for Throughput Processors," Ph.D. dissertation, UT Austin, 2021.
- [77] Y. Kim, V. Seshadri, D. Lee, J. Liu, and O. Mutlu, "A Case for Subarray-Level Parallelism (SALP) in DRAM," in *ISCA*, 2012.
- [78] V. Seshadri, Y. Kim, C. Fallin, D. Lee, R. Ausavarungnirun, G. Pekhimenko, Y. Luo, O. Mutlu, P. B. Gibbons, M. A. Kozuch, and T. Mowry, "RowClone: Fast and Energy-Efficient In-DRAM Bulk Data Copy and Initialization," in *MICRO*, 2013.
- [79] K. K. Chang, D. Lee, Z. Chishti, A. R. Alameldeen, C. Wilkerson, Y. Kim, and O. Mutlu, "Improving DRAM Performance by Parallelizing Refreshes with Accesses," in *HPCA*, 2014.
- [80] A. Olgun, H. Hassan, A. G. Yaglikci, Y. C. Tugrul, L. Orosa, H. Luo, M. Patel, E. Oguz, and O. Mutlu, "DRAM Bender: An Extensible and Versatile FPGA-based Infrastructure to Easily Test State-of-the-art DRAM Chips," *TCAD*, 2023.
- [81] SAFARI Research Group, "DRAM Bender - GitHub Repository," <https://github.com/CMU-SAFARI/DRAM-Bender>, 2022.
- [82] "Bittware XUPVH FPGA Board," <https://www.bittware.com/fpga/xup-vvh/>.
- [83] Xilinx Inc., "Xilinx Alveo U50 FPGA Board," <https://www.xilinx.com/products/boards-and-kits/alveo/u50.html>.
- [84] "Arduino MEGA Documentation," <https://docs.arduino.cc/hardware/mega-2560/>.
- [85] R. T. Smith, J. D. Chlipala, J. F. Bindels, R. G. Nelson, F. H. Fischer, and T. F. Mantz, "Laser Programmable Redundancy and Yield Improvement in a 64K DRAM," *JSSC*, 1981.

- [86] M. Horiguchi, "Redundancy Techniques for High-Density DRAMs," in *ISIS*, 1997.
- [87] B. Keeth and R. Baker, *DRAM Circuit Design: A Tutorial*. Wiley, 2001.
- [88] K. Itoh, *VLSI Memory Chip Design*. Springer, 2001.
- [89] J. Liu, B. Jaiyen, Y. Kim, C. Wilkerson, O. Mutlu, J. Liu, B. Jaiyen, Y. Kim, C. Wilkerson, and O. Mutlu, "An Experimental Study of Data Retention Behavior in Modern DRAM Devices," in *ISCA*, 2013.
- [90] V. Seshadri, T. Mullins, A. Boroumand, O. Mutlu, P. B. Gibbons, M. A. Kozuch, and T. C. Mowry, "Gather-Scatter DRAM: In-DRAM Address Translation to Improve the Spatial Locality of Non-Unit Strided Accesses," in *MICRO*, 2015.
- [91] S. Khan, D. Lee, and O. Mutlu, "PARBOR: An Efficient System-Level Technique to Detect Data-Dependent Failures in DRAM," in *DSN*, 2016.
- [92] S. Khan, C. Wilkerson, Z. Wang, A. R. Alameldeen, D. Lee, and O. Mutlu, "Detecting and Mitigating Data-Dependent DRAM Failures by Exploiting Current Memory Content," in *MICRO*, 2017.
- [93] D. Lee, S. Khan, L. Subramanian, S. Ghose, R. Ausavarungnirun, G. Pekhimenko, V. Seshadri, and O. Mutlu, "Design-induced Latency Variation in Modern DRAM Chips: Characterization, Analysis, and Latency Reduction Mechanisms," *POMACS*, 2017.
- [94] M. Patel, J. Kim, T. Shahroodi, H. Hassan, and O. Mutlu, "Bit-Exact ECC Recovery (BEER): Determining DRAM On-Die ECC Functions by Exploiting DRAM Data Retention Characteristics," in *MICRO*, 2020.
- [95] A. G. Yaglikci, M. Patel, J. S. Kim, R. Azizbarzoki, A. Olgun, L. Orosa, H. Hassan, J. Park, K. Kanellopoulos, T. Shahroodi, S. Ghose, and O. Mutlu, "BlockHammer: Preventing RowHammer at Low Cost by Blacklisting Rapidly-Accessed DRAM Rows," in *HPCA*, 2021.
- [96] A. van de Goor and I. Schanstra, "Address and Data Scrambling: Causes and Impact on Memory Tests," in *DELTA*, 2002.
- [97] K. Park, D. Yun, and S. Baeg, "Statistical Distributions of Row-hammering Induced Failures in DDR3 Components," *Microelectronics Reliability*, 2016.
- [98] K. Park, C. Lim, D. Yun, and S. Baeg, "Experiments and Root Cause Analysis for Active-precharge Hammering Fault in DDR3 SDRAM under  $3 \times \text{nm}$  Technology," *Microelectronics Reliability*, 2016.
- [99] H. Jun, J. Cho, K. Lee, H.-Y. Son, K. Kim, H. Jin, and K. Kim, "HBM (High Bandwidth Memory) DRAM Technology and Architecture," in *(IMW)*, 2017.
- [100] S. Mukherjee, *Architecture Design for Soft Errors*. Morgan Kaufmann Publishers Inc., 2008.
- [101] NVIDIA, "NVIDIA Tesla P100," <https://www.nvidia.com/en-us/data-center/resources/pascal-architecture-whitepaper>, 2016.
- [102] R. W. Hamming, "Error Detecting and Error Correcting Codes," *The Bell system technical journal*, 1950.
- [103] NVIDIA, "Dynamic Page Retirement," [https://docs.nvidia.com/deploy/pdf/Dynamic\\_Page\\_Retirement.pdf](https://docs.nvidia.com/deploy/pdf/Dynamic_Page_Retirement.pdf), 2019.
- [104] Apple Inc., "About the Security Content of Mac EFI Security Update 2015-001," <https://support.apple.com/en-us/HT204934>, 2015.
- [105] Hewlett-Packard Enterprise, "HP Moonshot Component Pack Version 2015.05.0," <http://h17007.www1.hp.com/us/en/enterprise/servers/products/moonshot/component-pack/index.aspx>, 2015.
- [106] Lenovo, "Row Hammer Privilege Escalation," [https://support.lenovo.com/us/en/product\\_security/row\\_hammer](https://support.lenovo.com/us/en/product_security/row_hammer), 2015.
- [107] Z. Greenfield and T. Levy, "Throttling Support for Row-Hammer Counters," 2016, U.S. Patent 9,251,885.
- [108] D.-H. Kim, P. J. Nair, and M. K. Qureshi, "Architectural Support for Mitigating Row Hammering in DRAM Memories," *IEEE CAL*, 2014.
- [109] K. S. Bains and J. B. Halbert, "Distributed Row Hammer Tracking," US Patent: 9,299,400, 2016.
- [110] K. Bains *et al.*, "Method, Apparatus and System for Providing a Memory Refresh," US Patent: 9,030,903, 2015.
- [111] Z. B. Aweke, S. F. Yitbarek, R. Qiao, R. Das, M. Hicks, Y. Oren, and T. Austin, "ANVIL: Software-Based Protection Against Next-Generation Rowhammer Attacks," in *ASPLOS*, 2016.
- [112] K. Bains *et al.*, "Row Hammer Refresh Command," US Patents: 9,117,544 9,236,110 10,210,925, 2015.
- [113] M. Son, H. Park, J. Ahn, and S. Yoo, "Making DRAM Stronger Against Row Hammering," in *DAC*, 2017.
- [114] S. M. Seyedzadeh, A. K. Jones, and R. Melhem, "Mitigating Wordline Crosstalk Using Adaptive Trees of Counters," in *ISCA*, 2018.
- [115] G. Irazoqui, T. Eisenbarth, and B. Sunar, "MASCAT: Stopping Microarchitectural Attacks Before Execution," *IACR Cryptology*, 2016.
- [116] J. M. You and J.-S. Yang, "MRLoc: Mitigating Row-Hammering Based on Memory Locality," in *DAC*, 2019.
- [117] E. Lee, I. Kang, S. Lee, G. E. Suh, and J. H. Ahn, "TWiCe: Preventing Row-Hammering by Exploiting Time Window Counters," in *ISCA*, 2019.
- [118] Y. Park, W. Kwon, E. Lee, T. J. Ham, J. H. Ahn, and J. W. Lee, "Graphene: Strong yet Lightweight Row Hammer Protection," in *MICRO*, 2020.
- [119] A. G. Yaglikci, J. S. Kim, F. Devaux, and O. Mutlu, "Security Analysis of the Silver Bullet Technique for RowHammer Prevention," arXiv:2106.07084, 2021.
- [120] I. Kang, E. Lee, and J. H. Ahn, "CAT-TWO: Counter-Based Adaptive Tree, Time Window Optimized for DRAM Row-Hammer Prevention," *IEEE Access*, 2020.
- [121] M. Qureshi, A. Rohan, G. Saileshwar, and P. J. Nair, "Hydra: Enabling Low-Overhead Mitigation of Row-Hammer at Ultra-Low Thresholds via Hybrid Tracking," in *ISCA*, 2022.
- [122] G. Saileshwar, B. Wang, M. Qureshi, and P. J. Nair, "Randomized Row-Swap: Mitigating Row Hammer by Breaking Spatial Correlation Between Aggressor and Victim Rows," in *ASPLOS*, 2022.
- [123] R. K. Konoth, M. Oliverio, A. Tatar, D. Andriesse, H. Bos, C. Giuffrida, and K. Razavi, "ZebRAM: Comprehensive and Compatible Software Protection Against Rowhammer Attacks," in *OSDI*, 2018.
- [124] S. Vig, S. Bhattacharya, D. Mukhopadhyay, and S.-K. Lam, "Rapid Detection of Rowhammer Attacks Using Dynamic Skewed Hash Tree," in *HASP*, 2018.
- [125] M. J. Kim, J. Park, Y. Park, W. Doh, N. Kim, T. J. Ham, J. W. Lee, and J. H. Ahn, "Mithril: Cooperative Row Hammer Protection on Commodity DRAM Leveraging Managed Refresh," in *HPCA*, 2022.
- [126] G.-H. Lee, S. Na, I. Byun, D. Min, and J. Kim, "CryoGuard: A Near Refresh-Free Robust DRAM Design for Cryogenic Computing," in *ISCA*, 2021.
- [127] M. Marazzi, P. Jattke, F. Solt, and K. Razavi, "REGA: Scalable Rowhammer Mitigation with Refresh-Generating Activations," in *S&P*, 2022.
- [128] Z. Zhang, Y. Cheng, M. Wang, W. He, W. Wang, S. Nepal, Y. Gao, K. Li, Z. Wang, and C. Wu, "SoftTRR: Protect Page Tables against Rowhammer Attacks using Software-only Target Row Refresh," in *USENIX ATC*, 2022.
- [129] B. K. Joardar, T. K. Bletsch, and K. Chakrabarty, "Learning to Mitigate RowHammer Attacks," in *DATE*, 2022.
- [130] J. Juffinger, L. Lamster, A. Kogler, M. Eichlseder, M. Lipp, and D. Gruss, "CSI: Rowhammer—Cryptographic Security and Integrity against Rowhammer (to appear)," in *S&P*, 2023.
- [131] A. G. Yaglikci, A. Olgun, M. Patel, H. Luo, H. Hassan, L. Orosa, O. Ergin, and O. Mutlu, "HiRA: Hidden Row Activation for Reducing Refresh Latency of Off-the-Shelf DRAM Chips," in *MICRO*, 2022.
- [132] A. Saxena, G. Saileshwar, P. J. Nair, and M. Qureshi, "AQUA: Scalable Rowhammer Mitigation by Quarantining Aggressor Rows at Runtime," in *MICRO*, 2022.
- [133] S. Enomoto, H. Kuzuno, and H. Yamada, "Efficient Protection Mechanism for CPU Cache Flush Instruction Based Attacks," *IEICE Transactions on Information and Systems*, 2022.
- [134] E. Manzhosov, A. Hastings, M. Pancholi, R. Piersma, M. T. I. Ziad, and S. Sethumadhavan, "Revisiting Residue Codes for Modern Memories," in *MICRO*, 2022.
- [135] S. M. Ajorpez, D. Moghimi, J. N. Collins, G. Pokam, N. Abu-Ghazaleh, and D. Tullsen, "EVAX: Towards a Practical, Pro-active & Adaptive Architecture for High Performance & Security," in *MICRO*, 2022.
- [136] A. Naseradini, M. Berger, M. Sammartino, and S. Xiong, "ALARM: Active Learning of Rowhammer Mitigations," <https://users.sussex.ac.uk/~mfb21/rh-draft.pdf>, 2022.
- [137] B. K. Joardar, T. K. Bletsch, and K. Chakrabarty, "Machine Learning-based Rowhammer Mitigation," *TCAD*, 2022.
- [138] H. Hassan, A. Olgun, A. G. Yaglikci, H. Luo, and O. Mutlu, "A Case for Self-Managing DRAM Chips: Improving Performance, Efficiency, Reliability, and Security via Autonomous In-DRAM Maintenance Operations," arXiv:2207.13358, 2022.
- [139] Z. Zhang, Z. Zhan, D. Balasubramanian, B. Li, P. Volgyesi, and X. Koutsoukos, "Leveraging EM Side-Channel Information to Detect Rowhammer Attacks," in *S&P*, 2020.
- [140] K. Loughlin, S. Saroiu, A. Wolman, and B. Kasicki, "Stop! Hammer Time: Rethinking Our Approach to Rowhammer Mitigations," in *HotOS*, 2021.
- [141] F. Devaux and R. Ayrignac, "Method and Circuit for Protecting a DRAM Memory Device from the Row Hammer Effect," US Patent: 10,885,966, 2021.
- [142] J.-W. Han, J. Kim, D. Beery, K. D. Bozdog, P. Cuevas, A. Levi, I. Tain, K. Tran, A. J. Walker, S. V. Palayam, A. Arreghini, A. Furnémont, and M. Meyyappan, "Surround Gate Transistor With Epitaxially Grown Si Pillar and Simulation Study on Soft Error and Rowhammer Tolerance for DRAM," *IEEE TED*, 2021.
- [143] A. Fakhrazadehgan, Y. N. Patt, P. J. Nair, and M. K. Qureshi, "SafeGuard: Reducing the Security Risk from Row-Hammer via Low-Cost Integrity Protection," in *HPCA*, 2022.
- [144] S. Saroiu, A. Wolman, and L. Cojocar, "The Price of Secrecy: How Hiding Internal DRAM Topologies Hurts Rowhammer Defenses," in *IRPS*, 2022.
- [145] S. Saroiu and A. Wolman, "How to Configure Row-Sampling-Based Rowhammer Defenses," *DRAMSec*, 2022.
- [146] K. Loughlin, S. Saroiu, A. Wolman, Y. A. Manerkar, and B. Kasicki, "MOESI-Prime: Preventing Coherence-Induced Hammering in Commodity Workloads," in *ISCA*, 2022.
- [147] R. Zhou, S. Tabrizchi, A. Roohi, and S. Angizi, "LT-PIM: An LUT-Based Processing-in-DRAM Architecture With RowHammer Self-Tracking," *IEEE CAL*, 2022.
- [148] S. Hong, D. Kim, J. Lee, R. Oh, C. Yoo, S. Hwang, and J. Lee, "DSAC: Low-Cost Rowhammer Mitigation Using In-DRAM Stochastic and Approximate Counting Algorithm," arXiv:2302.03591, 2023.
- [149] M. Marazzi, F. Solt, P. Jattke, K. Takashi, and K. Razavi, "ProTRR: Principled yet Optimal In-DRAM Target Row Refresh," in *S&P*, 2023.
- [150] A. Di Dio, K. Koning, H. Bos, and C. Giuffrida, "Copy-on-Flip: Hardening ECC Memory Against Rowhammer Attacks," in *NDSS*, 2023.
- [151] S. Sharma, D. Sanyal, A. Mukhopadhyay, and R. H. Shaik, "A Review on Study of Defects of DRAM-RowHammer and Its Mitigation," *Journal For Basic Sciences*, 2022.
- [152] J. Woo, G. Saileshwar, and P. J. Nair, "Scalable and Secure Row-Swap: Efficient and Safe Row Hammer Mitigation in Memory Systems," in *HPCA*, 2023.
- [153] J. H. Park, S. Y. Kim, D. Y. Kim, G. Kim, J. W. Park, S. Yoo, Y.-W. Lee, and M. J. Lee, "RowHammer Reduction Using a Buried Insulator in a Buried Channel Array Transistor," *IEEE Transactions on Electron Devices*, 2022.
- [154] M. Wi, J. Park, S. Ko, M. J. Kim, N. S. Kim, E. Lee, and J. H. Ahn, "SHADOW: Preventing Row Hammer in DRAM with Intra-Subarray Row Shuffling," in *HPCA*, IEEE, 2023.
- [155] W. Kim, C. Jung, S. Yoo, D. Hong, J. Hwang, J. Yoon, O. Jung, J. Choi, S. Hyun, M. Kang *et al.*, "A 1.1 V 16Gb DDR5 DRAM with Probabilistic-Aggressor Tracking, Refresh-

- Management Functionality, Per-Row Hammer Tracking, a Multi-Step Precharge, and Core-Bias Modulation for Security and Reliability Enhancement,” in *ISSCC*, IEEE, 2023.
- [156] C. Gude Ramarao, K. T. Kumar, G. Ujjinappa, and B. V. D. Naidu, “Defending SoCs with FPGAs from Rowhammer Attacks,” *Material Science*, 2023.
- [157] K. Guha and A. Chakrabarti, “Criticality based Reliability from Rowhammer Attacks in Multi-User-Multi-FPGA Platform,” in *VLSID*, IEEE, 2022.
- [158] L. France, F. Bruguier, M. Mushtaq, D. Novo, and P. Benoit, “Modeling Rowhammer in the gem5 Simulator,” in *CHES 2022-Conference on Cryptographic Hardware and Embedded Systems*, 2022.
- [159] L. France, F. Bruguier, D. Novo, M. Mushtaq, and P. Benoit, “Reducing the Silicon Area Overhead of Counter-Based Rowhammer Mitigations,” in *18th CryptArch Workshop*, 2022.
- [160] T. Bennett, S. Saroiu, A. Wolman, and L. Cojocar, “Panopticon: A Complete In-DRAM Rowhammer Mitigation,” in *DRAMSec*, 2021.
- [161] K. Arkan, A. Palumbo, L. Cassano, P. Reviriego, S. Pontarelli, G. Bianchi, O. Ergin, and M. Ottavi, “Processor security: Detecting microarchitectural attacks via count-min sketches,” *VLSI*, 2022.
- [162] C. Tomita, M. Takita, K. Fukushima, Y. Nakano, Y. Shiraishi, and M. Morii, “Extracting the secrets of openssl with rambleed,” *Sensors*, 2022.
- [163] A. Saxena, G. Saileshwar, J. Juffinger, A. Kogler, D. Gruss, and M. Qureshi, “PT-Guard: Integrity-Protected Page Tables to Defend Against Breakthrough Rowhammer Attacks,” in *DSN*, 2023.
- [164] R. Zhou, S. Ahmed, A. S. Rakin, and S. Angizi, “DNN-Defender: An in-DRAM Deep Neural Network Defense Mechanism for Adversarial Weight Attack,” arXiv:2305.08034, 2023.
- [165] A. Olgun, M. Osseiran, A. G. Yaglikci, Y. C. Tugrul, H. Luo, S. Rhyner, B. Salami, J. Gomez Luna, and O. Mutlu, “An Experimental Analysis of RowHammer in HBM2 DRAM Chips,” in *DSN Disrupt*, 2023.
- [166] C. Lim, K. Park, and S. Baeg, “Active Precharge Hammering to Monitor Displacement Damage Using High-Energy Protons in 3x-nm SDRAM,” *TNS*, 2017.
- [167] S.-W. Ryu, K. Min, J. Shin, H. Kwon, D. Nam, T. Oh, T.-S. Jang, M. Yoo, Y. Kim, and S. Hong, “Overcoming the Reliability Limitation in the Ultimately Scaled DRAM using Silicon Migration Technique by Hydrogen Annealing,” in *IEDM*, 2017.
- [168] D. Yun, M. Park, C. Lim, and S. Baeg, “Study of TID Effects on One Row Hammering using Gamma in DDR4 SDRAMs,” in *IRPS*, 2018.
- [169] C. Lim, K. Park, G. Bak, D. Yun, M. Park, S. Baeg, S.-J. Wen, and R. Wong, “Study of Proton Radiation Effect to Row Hammer Fault in DDR4 SDRAMs,” *Microelectronics Reliability*, 2018.
- [170] S. S. Nabavi Larimi, B. Salami, O. S. Unsal, A. C. Kestelman, H. Sarbazi-Azad, and O. Mutlu, “Understanding Power Consumption and Reliability of High-Bandwidth Memory with Voltage Underscaling,” in *DATE*, 2021.
- [171] J. Kwon, S.-J. Wen, R. Fung, and S. Baeg, “Temperature Estimation of HBM2 Channels with Tail Distribution of Retention Errors in FPGA-HBM2 Platform,” *Electronics*, 2023.
- [172] M. B. Sullivan, N. Saxena, M. O’Connor, D. Lee, P. Racunas, S. Hukerikar, T. Tsai, S. K. S. Hari, and S. W. Keckler, “Characterizing And Mitigating Soft Errors in GPU DRAM,” in *MICRO*, 2021.